

TALLINN UNIVERSITY OF TECHNOLOGY
DOCTORAL THESIS
64/2019

Analysis and Design Optimisation of Glass Structures

ERKO ÕUNAPUU



TALLINN UNIVERSITY OF TECHNOLOGY

School of Engineering

Department of Mechanical and Industrial Engineering

This dissertation was accepted for the defence of the degree 18/11/2019

Supervisor:

Professor Jüri Majak
School of Engineering
Tallinn University of Technology
Tallinn, Estonia

Co-supervisor:

Professor Martin Eerme
School of Engineering
Tallinn University of Technology
Tallinn, Estonia

Opponents:

Professor David Bassir
University of Bourgogne Franche-Comte
Besançon, France

Tõnu Leemet, PhD
Institute of Technology
Estonian University of Life Sciences
Tartu, Estonia

Defence of the thesis: 20/12/2019, Tallinn

Declaration:

Hereby I declare that this doctoral thesis, my original investigation and achievement, submitted for the doctoral degree at Tallinn University of Technology has not been submitted for doctoral or equivalent academic degree.

Erko Õunapuu



European Union
European Regional
Development Fund



Investing
in your future

signature

Copyright: Erko Õunapuu, 2019

ISSN 2585-6898 (publication)

ISBN 978-9949-83-507-2 (publication)

ISSN 2585-6901 (PDF)

ISBN 978-9949-83-508-9 (PDF)

TALLINNA TEHNIKAÜLIKOOL
DOKTORITÖÖ
64/2019

Klaaskonstruksioonide analüüs ning optimeerimine

ERKO ÕUNAPUU

**TAL
TECH**
KIRJASTUS

Contents

List of Publications	6
Author's Contribution to the Publications	7
Introduction	8
Abbreviations	10
1 Theoretical background	11
1.1 Glass structures	11
1.1.1 Float glass and its mechanical properties	11
1.1.2 Heat treatment and residual stress, treatment types, technology, collateral effects	12
1.1.3 Laminated glass	13
1.2 Optimisation methods in engineering design	14
1.2.1 Mathematical formulation of the optimization problem	14
1.2.2 Traditional gradient based methods	15
1.2.3 Discrete optimisation	17
1.2.4 Non-traditional, global optimisation	19
1.2.5 Hybrid methods	22
1.2.6 Multicriteria optimisation	23
1.3 Conclusions	26
1.4 Objectives of the research	27
1.5 Main hypotheses of the research	27
2 Experimental study	28
2.1 Glass layer and its properties	28
2.1.1 Acoustic method for measuring elasticity properties of the glass layer	28
2.1.2 Four-point bending test for measuring strength properties of the glass layer and laminate	30
2.2 Interlayer	32
2.3 Residual stresses in glass	33
3 Numerical modelling	37
3.1 Design of glass canopy panel	37
3.2 Modelling residual stresses in glass panel	40
3.2.1 Determination residual shear stresses in glass	40
3.2.2 Error estimation algorithm for residual normal stresses	43
3.2.3 Incorporating residual stresses in FEM model	43
4 Conclusion	47
References	49
Acknowledgements	53
Abstract	54
Lühikokkuvõte	55
Appendix	57
Curriculum vitae	90
Elulookirjeldus	91

List of Publications

- I E. Õunapuu, T. Velsker, M. Eerme. (2015). Design optimization of glass canopy panel subjected to snow load. Proceedings of the 10th International DAAAM Baltic Conference “INDUSTRIAL ENGINEERING” (pp. 104–108). Tallinn: Tallinn University of Technology.
- II K. Väer, J. Anton, A. Klauson, M. Eerme, E. Õunapuu, P. Tšukrejev. (2017). Material Characterization for Laminated Glass Composite Panel. Journal of Achievements in Materials and Manufacturing Engineering, 81, 11–17.
- III E. Õunapuu, J. Anton, A. Klauson. Modelling residual stresses in glass structures. AIP Conference Proceedings 2116, 330007 (2019).
- IV Majak, J.; Anton, J.; Õunapuu, E.; Auriemma, F.; Pohlak, M.; Eerme, M.; Klauson, A. (2019). Experimental Evaluation and Numerical Modelling Residual Stresses in Glass Panel. MATEC Web Conferences; 253.

Author's Contribution to the Publications

Contribution to the papers in this thesis are:

- I Paper 1
Design optimisation. Finite element analysis. Composing article.
- II Paper 2
Experimental study in cooperation with GlasStress. Composing article.
- III Paper 3
Theoretical review. Experimental study in cooperation with GlasStress. Development of finite element model.
- IV Paper 4
Experimental study in cooperation with GlasStress. Development of finite element model. Composing article.

Introduction

Glass is an aesthetical building material which utilisation is wider with every passing year. Curtain wall facades and smaller architectural elements like glass barriers and roofs are becoming more common as the material science and engineering is developing. This progress demands more precise methods and practices to construct safe buildings. The current study aims to investigate these issues.

The approaches proposed in the current study utilise methods and tools like design of experiment, global optimisation methods advanced finite element analysis, etc. The study is divided into four chapters. The first chapter gives an overview of the glass structures and optimisation methods used in engineering design. The second chapter include experimental study covering material characterisation of the layers of laminated glass panel (glass layer and interlayer), also measurement of the residual stress in glass. The third chapter focuses on numerical analysis and simulation. Herein two case studies are included: design optimisation of the glass canopy panel and modelling residual stresses in glass. The conclusion is given in chapter four.

The current thesis is based on four research papers presented in the list of publications. In the text the papers are referred as “Paper 1”, “Paper 2”, “Paper 3” and “Paper 4”.

Main goal of the current study is to develop the methodology for an accurate analysis and design of glass panels and laminated glass composite panels. In order to achieve the posed goal and all sub-objectives, the following activities have been performed:

Activity 1:

Experimental study for evaluation of the stiffness properties of the glass layer and interlayer.

Activity 2:

Development of methodology for evaluation of the plane residual stress tensor. The measurement of normal residual stresses and determination of the shear stress component by solving design optimisation problem.

Activity 3:

Development of strategy/methodology for integration residual stresses in FEM model.

Activity 4:

An advanced optimisation methods and tools have been employed for analysis of glass structures.

The novelties of the current study can be pointed out as

- An approach based on combining experimental study, theoretical and numerical analysis for design and analysis of the glass structures is proposed.
- The algorithm is developed for determining the shear stress component of the plane stress tensor.
- The error estimating algorithm has been developed for of the experimentally measured residual normal stresses.

- Two approaches have been proposed for integration residual stresses in FEM model.

The results obtained in the current study have been published in peer-reviewed journal papers and presented in several conferences.

Abbreviations

ACO	Ant Colony Optimisation
ANN	Artificial Neural Network
DE	Differential Evolution
DOE	Design of Experiments
EVA	Ethylene-Vinyl Acetate
EP	Ecolutionary Programming
FE	Finite Element
FEA	Finite Element Analysis
FEM	Finite Element Method
FG	Float Glass
GA	Genetic Algorithm
HGA	Hybrid Genetic Algorithm
HS	Heat Strengthened Glass
LGP	Laminated Glass Panel
PET	Polyethylene Tetraphthalate
PSO	Particle Swarm Optimisation
PVB	Polyvinul Putyral
SA	Simulated Annealing

1 Theoretical background

Modern day glass applications challenge engineers increasingly to utilise precise methods and solutions. Construction and automotive industry are the main fields where glass is more than window material allowing light to pass. High-rise buildings, galleries, and other conspicuous constructions demand from glass more than to pass light (Figure 1.1). Such applications require glass to act as load bearing element. Glass canopies, railings, beams and trusses employ heat treated glass which is stronger than the ordinary float glass. Such treatment raises different problems for architects and engineers. The current study proposes different methods and approaches to solve some of these issues.



Figure 1.1. Examples of glass structures

1.1 Glass structures

The development of architecture has transformed glass from simple infill material into one of the most important materials in modern city skyline. Not only larger glass areas for greater light passing, but modern architecture utilises glass as a load carrying material. Glass canopies, railings, bridges and full galleries and storm porches are conventional in contemporary urban architecture.

As the strength of conventional sheet glass is insufficient for afore-mentioned applications, heat treatment is utilised as a strengthening measure. Heat treating the glass increases its ultimate bending stress 5-6 times (Fröling, 2009, 2013) allowing it to employ in more demanding structures. Such heat treatment leaves the glass in prestressed state that requires researchers and engineers to expand the field of simulations and advanced numerical modelling.

1.1.1 Float glass and its mechanical properties

Glass as a construction material is generally utilised as a sheet. The thickness of the sheet varies, but the production process is the same. Common commercial glass is soda lime glass which chemical composition is shown in Table 1.1.

Table 1.1. Chemical composition of soda lime glass (Pfaender, 1996)

SiO ₂ [%]	Na ₂ O [%]	CaO [%]
70–75	12–16	10–15

The float glass (FG) process was invented in the 1950s in response to a pressing need for an economical method to create flat glass for automotive and architectural applications. Figure 1.2 shows the basic layout of the float glass line. The raw material

mass is heated in the furnace to $\sim 1550\text{--}1600^\circ\text{C}$ to achieve good chemical homogeneity. From there the glass flows onto the tin bath. Due to the different densities of glass ($\sim 2.3\text{ g/cm}^3$) and tin ($\sim 6.5\text{ g/cm}^3$) the glass ribbon floats on the tin. After cooling glass sheets with uniform thickness and flat surfaces are formed (Lorraine, 2016).

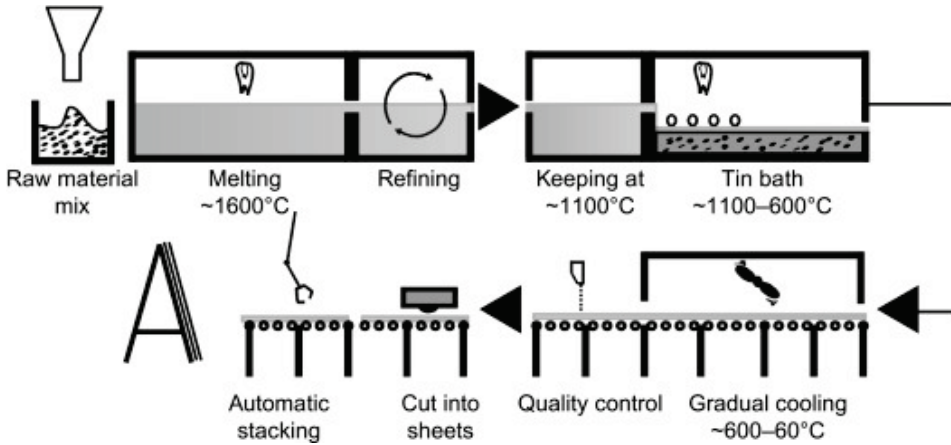


Figure 1.2. Schematic overview of a float glass process line (Achintha, 2016)

The general mechanical characteristics of the float glass are shown in Table 1.2.

Table 1.2 Mechanical properties of float glass (Nyonguè, 2016)

Elastic modulus [GPa]	Density [kg/m^3]	Poisson's ratio
70	2508	0.23

1.1.2 Heat treatment and residual stress, treatment types, technology, collateral effects

Due to the limited strength properties of float-glass the panel is heat-treated to obtain improved mechanical properties. After the process glass is in specific state with residual stresses.

Residual stresses – stresses introduced to in a material during processing, in the context of glass the stresses forming in thermal treatment (thermal stress). Compressive residual stresses deliberately introduced on the surface by the tempering of glasses improve their mechanical properties (Askeland et al, 2010).

The glass panel is heated in the oven and rapidly cooled down with air streams. The process causes the outer layers to compress (Figure 1.3; Wang et al., 2016). The mechanism is caused by the thermal expansion and elastic mismatch between the crystalline and glassy phases (Serbena & Zanotto, 2012).

To deform and brake such a glass the compressive stresses must be exceeded resulting in improved mechanical strength.

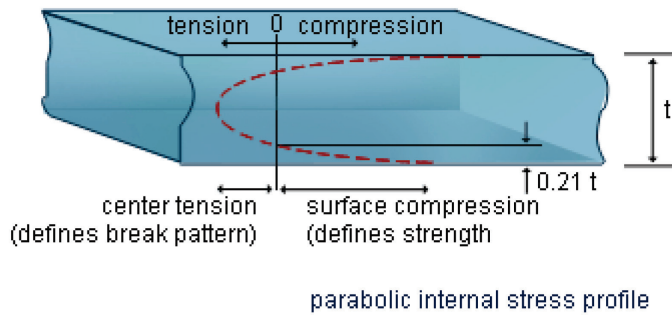


Figure 1.3. Compressive and tensile stress distribution in heat treated glass (Glass Academy, 2016)

Heat-strengthened (HS) glass has been subjected to a specifically controlled heating and cooling cycle and is generally twice as strong as annealed glass of the same thickness and configuration. Tempered glass is approximately four times stronger than regular annealed glass of the same thickness and configuration (Guardian Glass, 2019).

1.1.3 Laminated glass

Combining glass layers with different interlayers into laminated glass panel (LGP) improves different shortages of glass. Depending on the type the interlayer improves performance in sound insulation, safety and strength.

Glass as a laminated panel is a non-typical sandwich panel. Contrary to the classical sandwich the LGP has thick skins and thin core (Figure 1.4).

	Classical sandwich	vs	Laminated glass sandwich
Core	Thick, one layer		Thin, multilayer
Skin	Thin, multilayer		Thick, one layer (tempered glass)
Shear modulus of core	[10^{-2} ; 10^{-1}]		[10^{-5} ; 10^{-2}]
Shear modulus of skin			

Skin →

Core →

Skin →

Figure 1.4. Difference between classical sandwich and LGP

LGP is produced by joining two or more float or tempered glass sheets with one or more interlayers and by autoclaving the combination at 1400°C and at maximum pressure 14 bar (Achintha, 2016). Most common interlayer material is polyvinyl butyral (PVB) but also polyethylene tetraphthalate (PET), ethylene-vinyl acetate (EVA) are employed (Zhang, Hao, 2015.) Special purpose interlayer types may be utilised to achieve specific properties like thermal insulation solar control and sound reduction. (Yan & Shuxia, 2011).

One of the main reasons for the use of laminated glass in building envelopes is its safe failure mode compared to that of float glass and tempered glass. Recent developments include high-tech ionoplastic interlayers. According to the manufacturers, laminated glass with ionoplastic is lighter and stronger than conventional laminated glass, and can withstand storms, impacts and powerful blasts. (Dupont, 2015) Another actual application area of LGP's is solar panel manufacturing industry. (Naumenko & Eremeyev, 2014; Eisenträger et al, 2015).

1.2 Optimisation methods in engineering design

Before discussing the solution methods, it is needed to introduce the mathematical formulation of the optimisation problem.

1.2.1 Mathematical formulation of the optimization problem

In the case of single objective function, the optimisation problem can be formulated as

$$f(\bar{x}) \rightarrow \min, \quad (1.1)$$

subjected to constraints in form of equalities and/or inequalities, also bounds on design variables

$$h_k(\bar{x}) = 0, (k = 1 \dots l), \quad (1.2)$$

$$g_j(\bar{x}) \leq 0, (j = 1 \dots m), \quad (1.3)$$

$$x_i^{low} \leq x_i \leq x_i^{up}; i = 1 \dots n, \quad (1.4)$$

where \bar{x} is a vector of design variables x_i . In general, the objective function and/or constraints may be nonlinear. The lower and upper limits of design variables x_i^{low} and x_i^{up} define n-dimensional design space. In the case of multicriteria optimisation the constraints can be used in form (1.2)–(1.3), but instead of objective $f(\bar{x})$ here is a number of objectives $F_1(\bar{x}), \dots, F_s(\bar{x})$, responsible for the stiffness and strength characteristics, cost and life expectancy of the structure, information and energy consumption characteristics, etc. Note that some of the functions $F_i(\bar{x})$ may be subjected to minimisation (cost, energy consumption) and some to maximisation (stiffness, strength). Furthermore, the dimensions and magnitudes of the functions $F_i(\bar{x})$ may differ substantially. For that reason, as rule, the functions $F_i(\bar{x})$ are normalised as (Herranen et al., 2018)

$$f_i(\bar{x}) = \frac{\max F_i(\bar{x}) - F_i(\bar{x})}{\max F_i(\bar{x}) - \min F_i(\bar{x})}, \quad (1.5)$$

$$f_i(\bar{x}) = \frac{F_i(\bar{x}) - \min F_i(\bar{x})}{\max F_i(\bar{x}) - \min F_i(\bar{x})}. \quad (1.6)$$

The formulas (1.5) and (1.6) are applied to functions subjected to maximisation and minimisation, respectively. Thus, as a result all normalised functions $f_i(\bar{x})$ are subjected to minimisation. Furthermore, it can be seen from (5)–(6), that $f_i(\bar{x})$ remains in interval [0,1] when $\min F_i(\bar{x}) \leq F_i(\bar{x}) \leq \max F_i(\bar{x})$. Since the minimum and maximum values of the objective $\min F_i(\bar{x})$ and $\max F_i(\bar{x})$ are not known but estimated values,

the values of the $f_i(\bar{x})$ may not rely strictly in interval [0,1]. Finally, the normalised objective functions, corresponding to multicriteria optimisation can be presented as

$$f(\bar{x}) = (f_1(\bar{x}), f_2(\bar{x}), f_3(\bar{x}) \dots, f_n(\bar{x})) \rightarrow \min. \quad (1.7)$$

The objective function (1.7) together with constraints in form of equalities and/or inequalities (1.2)–(1.3) and bounds on design variables (1.4) represent mathematical formulation of multicriteria optimisation problem.

The aim of following sections is to give an overview of mathematical methods used widely in engineering design. Due to conciseness sake certain selection of methods should be done. The optimisation methods can be classified as traditional methods (as rule gradient based), discrete optimisation methods, global optimisation methods (most commonly population based) and hybrid methods (as a rule contain combination of global and local search methods). In the case of complex problems, the solution of the initial optimisation problem is divided into multiple simpler subproblems i.e. decomposition method is applied. In latter case the optimisation procedure has often hierarchical structure.

1.2.2 Traditional gradient based methods

Despite to a number of shortcomings and limitations (will be discussed below) the traditional gradient based methods are still widely used in engineering design. The main reason – if applicable, the gradient methods are computationally cheap in comparison with evolutionary etc. methods.

In general, the gradient based methods begin with an initial guess and iteratively refines it so as to asymptotically approach the optimum. Let us assume that function $f(x^1)$ is subjected to minimisation and x^0 stand for initial point, then the solution method seeks an update x^1 , which satisfies $f(x^1) < f(x^0)$, next for update x^2 , which satisfies $f(x^2) < f(x^1)$, as descent condition etc. The update of the design variable can be given by the following rule (Iqbal, 2013)

$$x^{n+1} = x^n + \gamma_n d_n, \quad (1.8)$$

where d_n and γ_n stand for search direction and the step size, respectively. Thus, the iterative method consists from the following two basic steps:

- 1) Finding the suitable search direction d_n along which the objective function value locally decreases, and any constraints are obeyed,
- 2) Performing line search along d_n to find x^{n+1} such that $f(x^{n+1})$ attains its minimum value.

In the following are outlined three well known gradient methods used in engineering design.

Steepest Descent Method

The steepest descent (also gradient descent) method can be considered as a simplest widely used gradient method. According to this method the d_n is determined by maximum decrease in the function values i.e. the antigradient vector at the current point n (Iqbal, 2013). Thus,

$$d_n = -\nabla f(x^n), \quad (1.9)$$

and the relation (1.8) can be rewritten as

$$x^{n+1} = x^n - \gamma_n \nabla f(x^n). \quad (1.10)$$

The step size γ_n is determined so that $f(x^n - \gamma_n \nabla f(x^n))$ attains minimum value. For example, if the Hess matrix can be computed i.e. the second order derivatives exists, the γ_n can be evaluated as

$$\gamma_n = \frac{g_n^T g_n}{g_n^T H_n g_n}, \quad (1.11)$$

where g_n is gradient ($g_n = \nabla f(x^n)$) and H_n is the Hess matrix in step n

$$H(x) = \begin{bmatrix} \frac{\partial^2 f}{\partial x_1^2} & \frac{\partial^2 f}{\partial x_1 \partial x_2} & \cdots & \frac{\partial^2 f}{\partial x_1 \partial x_n} \\ \frac{\partial^2 f}{\partial x_2 \partial x_1} & \frac{\partial^2 f}{\partial x_2^2} & \cdots & \frac{\partial^2 f}{\partial x_2 \partial x_n} \\ \cdots & \cdots & \cdots & \cdots \\ \frac{\partial^2 f}{\partial x_n \partial x_1} & \frac{\partial^2 f}{\partial x_n \partial x_2} & \cdots & \frac{\partial^2 f}{\partial x_n^2} \end{bmatrix}, \quad (1.12)$$

The implementation of the 2D steepest descent method is shown in Figure 1.5.

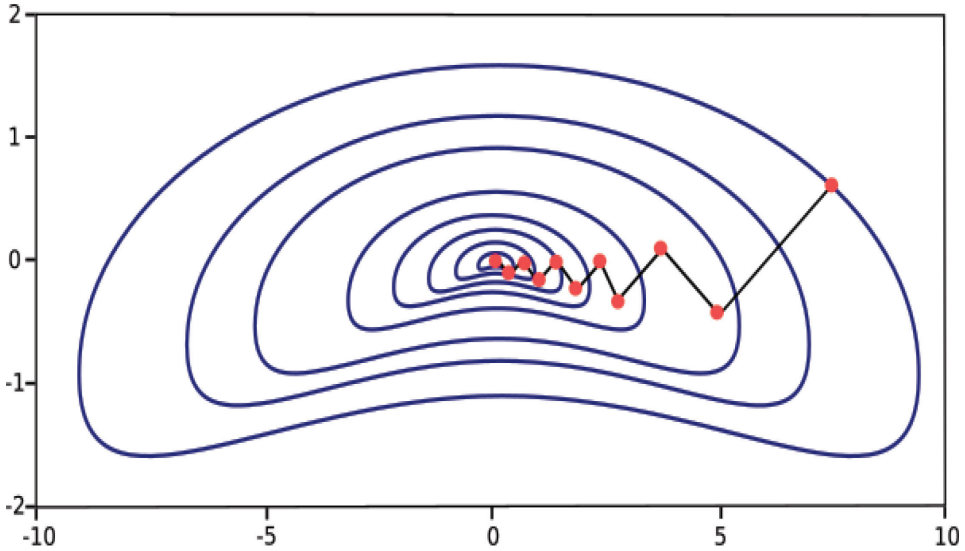


Figure 1.5. Implementation of steepest descent method, training neural network (Quesada)

It can be seen from the Figure 1.5 that the step size is vanishing. Without Hess matrix the step size can be computed as

$$\gamma_n = \frac{g_n^T g_n \hat{\gamma}^2}{2(\hat{f} - f(x_n) + \hat{\gamma} g_n^T g_n)}, \quad (1.13)$$

where

$$\hat{\gamma} = \gamma_{n-1}, \quad \hat{f} = f(x_n - \hat{\gamma} g_n), \quad (1.14)$$

Latter formulas are applicable when the objective function is differentiable only one time.

Newton's Method

First it should be noted that the Newton method is most widely known for solving algebraic equations. Herein the Newton's method is considered for optimisation. In the case of Newton's method, the update of the design variable can be performed as

$$x_{n+1} = x_n - \gamma_n H_n^{-1} g_n. \quad (1.15)$$

The Newton method converges faster in comparison with steepest descent method (second order convergence) but needs better initial solution to converge at all. In classical Newton method the step size γ_n is taken equal to one. The computations by formula (1.15) can be performed up to the gradient is less than ε (given value, depend on accuracy requirements for particular problem) or difference between to sequential values of x satisfy the condition $|x_{n+1} - x_n| < \varepsilon$. Note that, the convergence is not guaranteed - it depends on starting point used. For this reason, in numerical algorithms, it is suggested to use some loop control variable and interrupt computations when this variable attains its upper limit value (this allow to avoid infinite loops).

Augmented Lagrange multipliers method

The Lagrange multipliers method exploits gradient, but its general working principle differs from above described gradient methods. In the case of Lagrange multipliers method, the initial optimisation problem is converted to system of equations and then solved. Let us consider optimisation problem in form (1.1)–(1.4). The Lagrange function L , corresponding to considered optimisation problem, can be expressed as

$$L = f(x) + \sum_{k=1}^l \lambda_k h_k + \sum_{i=1}^m \mu_i g_i, \quad (1.16)$$

where λ_k and μ_i stand for the Lagrange multipliers of the constraint functions in form of equalities and inequalities, respectively. Equalising the strong variation of the Lagrange function to zero ($\nabla L = 0$), one obtains

$$\nabla f(x^*) + \sum_{i=1}^m \mu_i \nabla g_i(x^*) + \sum_{j=1}^l \lambda_j \nabla h_j(x^*) = 0, \quad (1.17)$$

$$h_k(x^*) = 0, (k = 1 \dots l), \mu_i g_i(x^*) = 0, \mu_i \geq 0, (i = 1 \dots m). \quad (1.18)$$

Solving the system of equations (1.17)–(1.18) one obtains the optimal solution x^* . The conditions (1.17)–(1.18) are known as Karush–Kuhn–Tucker necessary optimality conditions (Kuhn & Tucker, 1951). Thus, the conditions (1.17)–(1.18) can be checked also in the cases when any other gradient based method is applied.

1.2.3 Discrete optimisation

Obviously, the complex engineering design problems may involve integer or discrete variables. Based on literature the cutting plane methods are most widely used methods for discrete/integer programming. The basic steps of the cutting plane methods can be given as (Belegundu & Chandrupatla, 2012; Chong & Zak, 2013)

- Instead of integer programming problem is solved corresponding problem with real variables i.e. the variables are relaxed (relaxation method). If the obtained optimal solution appears integer, then the initial problem is solved.
- If the solution includes real valued variables, the linear constraints will be applied so that feasible integer solutions are available. The idea is to exclude non-integer solutions to the problem.

To explain the method, let us consider simple sample problem:

$$\begin{cases} 4x_1 + 6x_2 \rightarrow \min \\ 2x_1 + 2x_2 \geq 5 \\ x_1 - x_2 \leq 1 \\ x_1, x_2 \geq 0 \\ x_1, x_2 \text{ integer} \end{cases} \quad (1.19)$$

The solution of relaxed problem where x_1, x_2 may have real values gives solution where $x_1 = 1.75$ and $x_2 = 0.75$. Thus, by applying constraint on variable x_1 as shown in Figure 1.6 will eliminate real valued solutions in interval $x_1 \in (1, 2)$.

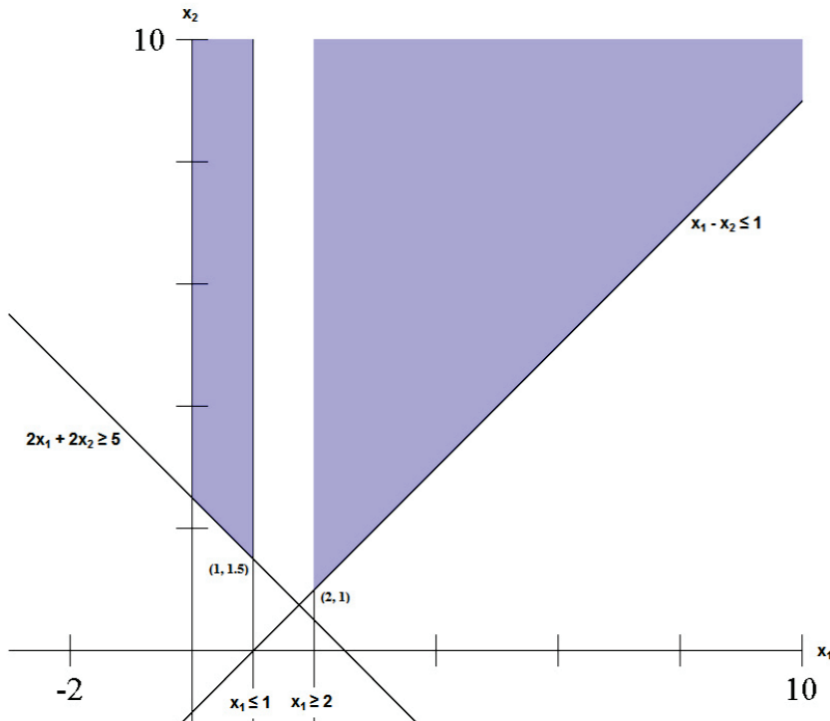


Figure 1.6. Cutting plane method. Adding constraint on variable x_1 (Smith & Taskin, 2008)

Depending on particular cutting plane methods and software used the solutions can be found separately or together for two separated domains. The relaxation and cutting may be applied iteratively up to all design variables will have integer values. The most widely used cutting plane method is branch and bound method.

1.2.4 Non-traditional, global optimisation

Since traditional optimisation methods cover poorly or do not cover certain needs of complex real-world engineering design problems (global optimum, mixed integer and discrete variables, etc) new non-traditional optimisation techniques are introduced, referred often as global optimisation methods. The non-traditional optimisation methods are inspired from nature (biological, physical structures and processes). Many nature-based methods and its variations are available in literature:

- genetic algorithms (GA) (Holland, 1975; Deb, 2000),
- particle swarm optimisation (PSO) (Kennedy & Eberhart, 1995),
- ant colony optimisation (ACO) (Dorigo, 1992),
- differential evolution (DE) (Storn & Price, 1997),
- simulated annealing (SA) (Reguera & Cortínez, 2016),
- evolutionary programming (EP) (Keller 2010; Zitzler & Thiele, 1999),
- Tabu search, etc (Glover, 1990).

In engineering design are dominating genetic algorithms, widely used are also other nature-based methods like PSO, DE and ACO. For these reasons in the following the working principles of GA are explained in more details, and PSO and ACO are described in brief.

Genetic algorithms

GA is inspired from by Charles Darwin's theory of natural evolution as common for population-based methods. Originally, the binary coding based GA, was introduced in (Holland, 1975). GA has three main encoding types (binary, real value and permutation) covering different problems (Deb, 2000; Sahman, et al., 2009). General flowchart of GA is depicted on Figure 1.7. First the initial population will be generated using random and applying rules, constraints depending on particular problem. Next, the fitness function is evaluated. Most commonly this is objective function or its normalised/converted form. The following three basic operators need more detailed description. First of them, the selection operator is responsible for selection individuals for reproduction. There are several selection rules available in literature like roulette wheel selection, rank selection, tournament selection, Boltzmann selection, etc. The simplest is the tournament selection according to which n individuals selected from population compete against each other and the individual with the highest fitness participates in crossover. However, this rule has drawback, diversity is preserved, since the individuals have equal chance to be selected for tournament.

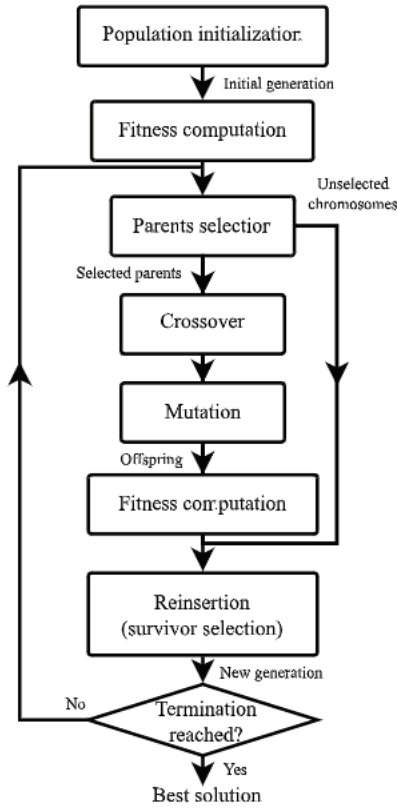


Figure 1.7. Flowchart of the GA (Vaissier et al., 2019)

One of most widely used selection method is the roulette wheel selection. Selection in this method is proportional to the fitness function of individual (Figure 1.8).

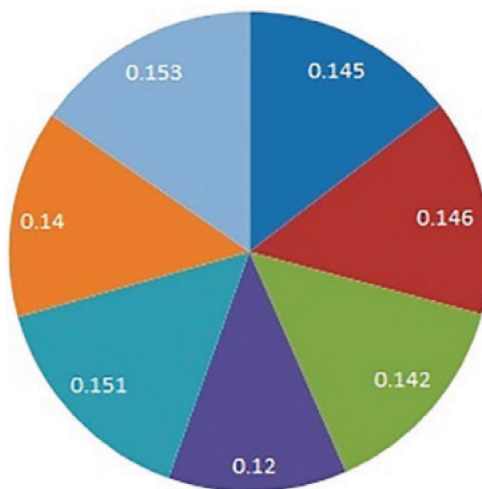


Figure 1.8. Roulette wheel selection (Chunka et al., 2018)

The probability of an individual being selected as a parent for crossover is given in (Jebari & Madiafi, 2013)

$$p(k) = \frac{f(k)}{\sum_{i=1}^N f(i)}. \quad (1.20)$$

In (1.20) $p(k)$ is the probability to be selected for individual k , $f(k)$ and N stand for fitness function and size of the population, respectively. Obviously, the probability of an individual being selected $p(k) \in [0,1]$. Thus, it is extremely simple to simulate computationally the wheel rotation – it can be generated just random number in interval $[0,1]$ and check to which sector it belongs. In crossover operator the selected individuals produce offsprings (children). The crossover scheme corresponding to binary coding is shown in Figure 1.9.

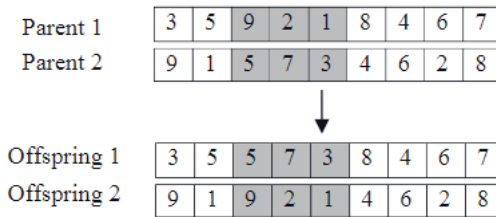


Figure 1.9. Double point cross-over operator (Arram & Ayob, 2019)

In Figure 1.9 here are two cross-over points. The first offspring get the first two data units from parent 1, next three data units from parent 2 and last four data units again from parent 1. The second offspring gets all data units not used for the first offspring. In the case of long chromosomes here may be used multiple point cross-over operators, where change of parents for selection of alleles for offspring is made multiple times. Also, the breakpoints (locations where parents are changed) are normally generated by random.

After crossover the chromosomes are subjected to mutation. The aim of mutations is to prevent convergence to local minimum. The mutation of a bit changing 0 to 1 and vice-versa. The mutation of chromosomes is performed with given mutation probability (mutation coefficient is commonly taken small like 0.005, since large mutation lead to perturbations, loss of convergence).

Next step is to compute fitness values for new mutated individuals (Figure 1.7). The reinsertion and following survival selection are performed based on values of the fitness functions, but also based on distance between individuals (too much similar individuals is not the best). Here in most of algorithms the size of population is kept constant. Finally, the termination condition is checked and if needed, the control is returned to selection operator. The termination condition may be given by number of generations, also values of convergence parameters, etc.

Particle swarm optimisation

PSO is based on simulating bird flocking, fish schooling or sociological behaviour of a group of people (Kennedy & Eberhart, 1995). The population of solutions is called swarm and individuals are called particles. First the random solutions (particles) are generated, where each particle has speed and coordinate for moving in d dimensional space. The flying is modified according to particles flying experience and that of other particles

present in the swarm. The particles have memory and each of them keeps track of its previous (local) best position (Marini & Walczak, 2015).

Differential evolution algorithm

DE can be considered as modification of GA (Storn & Price, 1997). The population is updated by adding the weighted difference between two population vectors to the third population vector. The main difference between GA and DE is that constructing better solutions in genetic algorithms rely on crossover, but in DE relies on mutation operator. The mutation operation is employed as a search mechanism and selection operation to direct the search toward the prospective domains. The non-uniform crossover utilised in DE allows to that offspring vector parameters from one parent more often than it does from others.

Ant colony optimisation

ACO is a genetic algorithm inspired by an ant's natural behaviour introduce in (Dorigo, 1992). The aim is to model the behaviour of ants searching an optimal path between their colony and a source of food (see Figure 1.10).

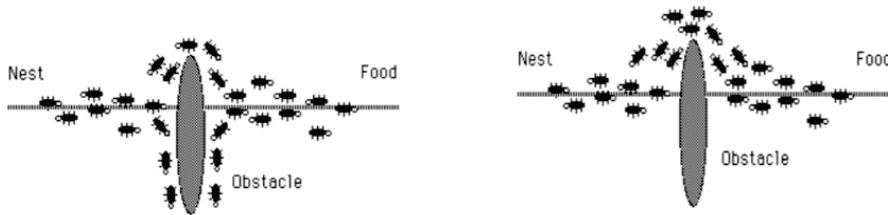


Figure 1.10. ACO, searching an optimal path between colony and a source of food (Santosa, 2015)

Basic principles of ACO can be outlined as:

- ants use pheromones to find the shortest path between home and food source
- pheromones evaporate quickly
- ants prefer to use shorter paths with denser pheromone.

In can be seen from Figure 1.10 that after certain training the initial longer path (left) has been replaced by shorter path (right).

1.2.5 Hybrid methods

As it can be assumed the hybrid methods are considered as combination of two or more optimisation methods. Obviously, many combinations are available. Herein are discussed some combinations used widely in engineering design. The general aim of the hybrid methods is to combine advantages of the methods it includes. Thus, in the case of complex engineering design problems it is reasonable to apply first selected global optimisation method (provide/assume convergence to global optimum) and then perform local search with gradient based etc. methods (provide fast convergence and avoid perturbations). One widely used method in engineering is hybrid genetic algorithm (HGA), where GA is combined with some gradient, etc. method. However, in the case of integer variables latter approach is not applicable and the GA can be combined with some integer programming methods like Hill climbing or branch and bound. In mainstream first is applied GA (global search) and then gradient, Hill, etc. method (local search). In Figure 1.11 is shown the convergence of the HGA to global optimum,

where first is applied GA and then for local reach Hill Climbing methods (Yun & Moon, 2003).

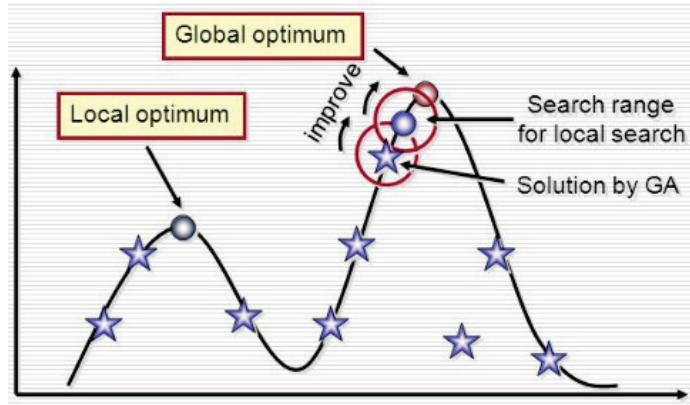


Figure 1.11. Convergence of HGA to global optimum, GA+Hill climbing (Yun & Moon, 2003)

This does not mean that GA cannot be used for local search, especially its modifications. For example, in (Martínez & Lozano, 2007) the GA is tuned for local search. PSO is combined often with SA (Javidrad, 2018), but also with GA (Allahyari et al., 2016; Vosoughi & Gerist, 2014). The hybrid algorithm found often use in hierarchical/multilevel optimisation (Ferreira et al., 2014; Herranen et al., 2018).

1.2.6 Multicriteria optimisation

In the case of multicriteria optimisation problems here are two or more functions subjected to minimisation/maximisation. The functions subjected to maximisation minimisation can be normalised according to (1.5) and (1.6), respectively. As results all objective function are subjected to minimisation and are in the same range. Thus, without restrictions, the multicriteria optimisation problem can be formulated as

$$f(\bar{x}) = [f_1(\bar{x}), f_2(\bar{x}), \dots, f_r(\bar{x})] \rightarrow \min, \quad (1.21)$$

subjected to constraints (1.2)–(1.4).

Based experience acquired in workgroup it can be mentioned that to start from selection of optimisation method is not the best choice. Preliminary analysis is necessary. First it is needed to select optimisation strategies

- to apply Pareto concept,
- to combine objectives to one and apply single criterion optimisation.

Latter selection is not always strict and needs additional work. Namely, it is reasonable to combine non-contradictive criteria into one and apply Pareto concept to contradictive criteria. The fact, that the two selected criteria are contradictive (or not), can be checked by performing preliminary pairwise analysis of criteria. Furthermore, latter work may be comprehensive if the number of criteria is large and here is needed to apply both strategies, since some criteria are contradictive and some not. However, omitting this preliminary study of optimality criteria may lead to incorrect/partial results.

Weight-based (Archimedean) approaches

The most widely use weight-based approach is obviously the weighted sum method. The reason why the weighted sum method is commonly used is its simplicity. According to weighted sum method the objective functions are combined in to one objective based of the following relations (Hajkowicz & Higgins, 2008)

$$f_{WSM} = \sum_{i=1}^r w_i f_i(\bar{x}) \rightarrow \min, \quad (1.22)$$

where the objective functions $f_i(\bar{x})$ are normalised according to formulas (1.5)–(1.6). The weights w_i characterise the importance of particular objective function and are subjected to the following constraints:

$$\sum_{i=1}^r w_i = 1, \quad 0 \leq w_i \leq 1. \quad (1.23)$$

After combining objective functions (1.21) the multicriteria optimisation problem is converted to single criterion optimisation and the above described methods for single criterion optimisation are applicable. The drawback of the weighted sum method is that it provides limited information in the case of contradictive objectives and that function (1.22) does not cover complex relations between objectives.

In order to cover more complex relations between objectives the weighted sum method has been generalised/upgraded to compromised programming method. In the case of latter method, the objectives are combined as

$$f_{CPM} = \left[\sum_{i=1}^r (w_i f_i) \right]^{c \frac{1}{c}}. \quad (1.24)$$

The coefficient c is the importance of maximal deviation. In the case $c > 1$ the deviations from ideal results are not penalised proportionally. The larger deviations are penalised more strictly (relation may be exponential etc.). In the case of $c = 1$ the compromise programming method reduces to the weighted summation method. Application of the compromise programming method is not substantially more complicated than weighted summation method, but it provides better results for problems where large deviation is critical (medicine, space applications, etc.). In (Majak et al., 2012) the weighted sum and compromise programming techniques are employed for design optimisation of car frontal protection systems, since the objectives considered, the peak force and difference between the maximal and the minimal force, appears not contradictory. There are number of other weight-based methods available. Herein are selected widely used methods in engineering design.

Pareto concept

The Pareto optimality concept for multicriteria optimisation was introduced by the French-Italian economist Vilfredo Pareto. The Pareto front allows to evaluate one objective against another (Mohammad, 2005). Pareto has made the famous observation that 20% of the population of Italy owned 80% of the property. The Pareto concept can be formulated as: a design is considered Pareto optimal if there does not exist any other design which improves the value of any of its objective criteria without deteriorating at

least one other criterion (Brisset & Gillon, 2015). The dominance between two solutions can be expressed as x_1 dominates x_2 if

$$f_i(x_1) \leq f_i(x_2) \quad (1.25)$$

for all objective functions

$$f_j(x_1) < f_j(x_2) \quad (1.26)$$

for at least one objective function.

A design x^* is said to be nondominated (Pareto optimal) if no other feasible design dominates it. The set of all non-dominated designs forms the Pareto front (Figure 1.12). This non-dominance principle leads to solution where the lowest points in graph should be connected (forming Pareto front) and the remaining points should be deleted. In (Aruniit et al., 2011) the design of particulate filled composite plastic materials from recycled glass fibre reinforced plastics was studied and the Pareto concept was applied for cost and combined function of mechanical characteristics. It was determined by the preliminary analysis that the mechanical characteristics (the elongation at break and tensile strength) are not in contradiction and thus, corresponding criteria were combined into one objective by utilising the weighted sum technique ($f = f_1 + f_2$). The obtained combined criterion appears in contradiction with cost, thus the Pareto concept was applied.

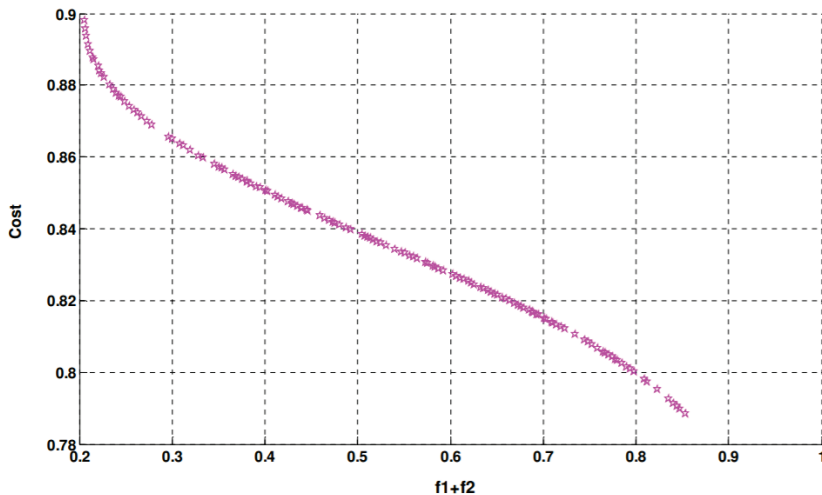


Figure 1.12. Pareto front. The combined objective ($f = f_1 + f_2$) versus cost f_3 (Aruniit et al., 2011)

Note, that each point in Pareto front is optimal solution. Thus, decision makers can use additional consideration for final decision like best available solution for given cost, etc. Obviously, the Pareto front gives valuable information and provide flexible possibilities for final choice. In practice often are selected points on Pareto front before sudden ascend.

It is interesting that the Pareto front may be also non-continuous. In (Herranen et al., 2011) the design and testing of sandwich structures with different core materials is studied. The material properties corresponding to different cores used in design were different and obviously not continuous. In this reason one obtains the following Pareto front (Figure 1.13).

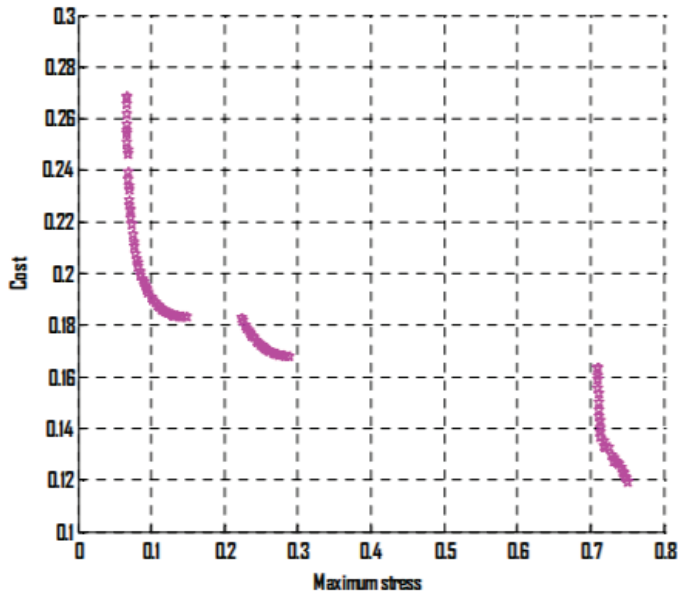


Figure 1.13. Maximum stress vs cost of the sandwich structure

Finally, here is possible that Pareto front contains one point or number of closed points only. This refer to the situations where the objective functions are not in contradiction and the use of Pareto concept is not justified (preliminary analysis is not carefully done).

1.3 Conclusions

In first chapter is given an overview on glass structures and optimisation methods used widely in engineering design.

Laminated glass composite panels can be considered as engineering structures with outstanding strength and stiffness properties. The viscoelastic/plastic interlayer used allows to attain high safety standards and sound absorbing properties.

In order to develop an accurate glass laminated composite plate analysis models, here is need to

- determine material properties of the glass layers and interlayer (non-destructive and mechanical tests),
- consider effect of residual stresses in glass (experimental determination, numerical modelling).

As rule the global optimisation methods need some featuring/tuning for particular problems (determining design space, population size, selection methods, mutation rate, elitism, etc.).

In the case of complex real world engineering design problems, which may include nonlinearity, mixed integer variables, constraints and etc. it is reasonable to employ global optimisation methods or hybrid methods where global optimisation is combined with some faster technique (gradient method, etc.) in order to find global optimum in

reasonable time. For structural optimisation problems the GA and PSO and most widely used (for general problems the priorities of the methods are not known).

In the case of simpler design problems, where gradient methods are applicable the Levenberg-Marquart method can be suggested (one of most widely used), since it combines the advantages of the steepest descent and Newton methods (wide convergence domain and fast convergence rate).

In the case of hybrid algorithm where global some optimisation technique is combined with gradient method, the time needed to global optimisation technique is several magnitudes higher, and thus the gradient method can be selected based on wider convergence domain.

In the case of multicriteria optimisation problems it is extremely important thoroughgoing preliminary analysis of the problem for selection right optimisation strategies, possible decomposition, simplification of the problem.

1.4 Objectives of the research

Main goal of the current study is to develop the methodology for an accurate analysis and design of glass panels and laminated glass composite panels. In order to achieve the posed goal and all sub-objectives, the following activities have been performed:

Activity 1: Experimental study for evaluation of the stiffness properties of the glass layer and interlayer.

Activity 2: Development of methodology for evaluation of the plane residual stress tensor. The measurement of normal residual stresses and determination of the shear stress component by solving design optimisation problem.

Activity 3: Development of strategy/methodology for integration residual stresses in FEM model.

Activity 4: An advanced optimisation methods and tools have been employed for analysis of glass structures.

1.5 Main hypotheses of the research

The main hypotheses of the current study can be pointed out as:

H1: The accuracy of the analysis models of the glass panels and laminated glass composites panel can be improved by taking account the effect of residual stresses.

H2: A simple and effective algorithm can be developed for estimation the value of the residual shear stress based on rotation formulas of the stress tensor and appropriately planned measuring of residual normal stresses.

H3: The error of the experimentally measured residual normal stress can be estimated as difference of the theoretical and experimental value.

H4: An advanced, global optimisation techniques based methods and tools can be utilised for design optimisation of laminated glass structures.

2 Experimental study

As mentioned above, for numerical modelling laminated glass composite panel, first the mechanical properties of the all layers should be determined. Additionally, the effect of residual stresses caused by high temperature applied during manufacturing process should be considered. In the following the experimental study performed for evaluation of the material properties of glass layers and interlayer is described. All tests except measuring residual stresses are performed in laboratories of Department of Mechanical and Industrial Engineering in the Tallinn University of Technology. The residual stresses of the glass have been measured in private company GlasStress Ltd.

2.1 Glass layer and its properties

Nowadays the sustainable approach should be implemented in experimental study if it is available. In the current study, the following two kind of tests have been performed for evaluating glass layer of the laminate:

- determining the stiffness properties (elastic properties),
- determining the strength properties.

The stiffness properties are determined using non-destructive testing without generating waste and strength properties using mechanical testing. The results from the test are expected to be similar to the values described in chapters 1.1.1 and 1.1.2.

2.1.1 Acoustic method for measuring elasticity properties of the glass layer

In the current study the glass layer is considered as an isotropic material. The isotropic material is characterised with two independent elastic material parameters which can be determined by an indirect method based on the measurement of longitudinal pressure wave (P-wave) and shear wave (S-wave) speeds in solid. The wave speed is determined by the measurement of the time of flight of the individual pulses of P- and S-waves between reflecting surfaces (Figure 2.1). Up to three repetitive tests have been performed.

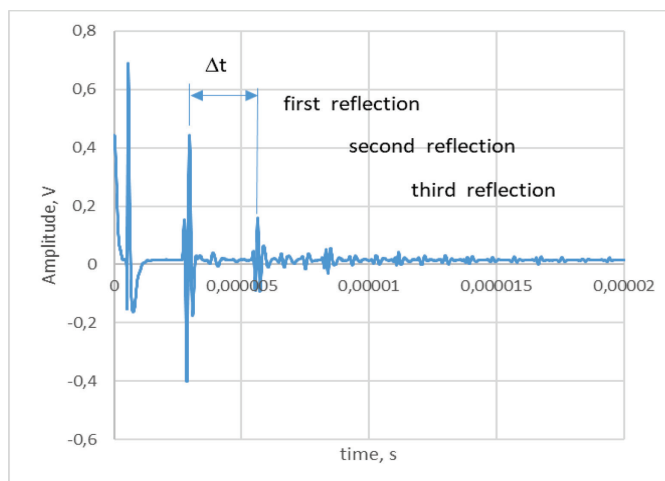


Figure 2.1. Measuring time of flight of the individual pulses of P-waves (Publication IV, 2019)

The time of flight of the individual pulses of P-waves between first and second reflection is denoted by Δt in Figure 2.1. The signal is generated by JSR DPR300 pulse generator (Figure 2.2).

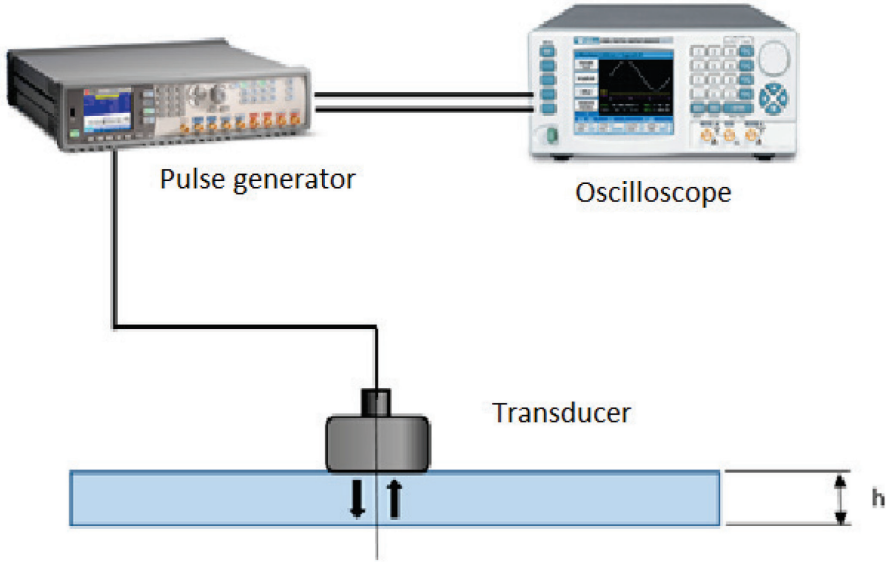


Figure 2.2. Set up for measuring P-wave and S-wave speeds (Publication IV, 2019)

Piezoelectric broadband contact transducer Olympus M110 (central frequency 5MHz) is utilised to generate P-wave and transducer V151 (central frequency 0.5MHz) to generate S-wave. Assuming, the density of the glass is known (Chapter 1.1.1), the bulk modulus M and shear modulus G can be computed as (2.1) (Auriemma, 2017).

$$M = c_p^2 \rho; G = c_s^2 \rho, \quad (2.1)$$

where ρ is a material density, respectively, c_p and c_s stand for the wave speeds of the P and S waves. In the case of isotropic material, the Young modulus E and Poisson ratio ν can be determined in terms of known bulk modulus M and shear modulus G (2.2) and (2.3) respectively (Auriemma, 2017).

$$E = \frac{G(3M - 4G)}{M - G}, \quad (2.2)$$

$$\nu = \frac{M - 2G}{2M - 2G}, \quad (2.3)$$

The measured pressure- and shear wave speeds, also the computed values of elastic properties of the glass layer are shown in Table 2.1 (Publication IV, 2019).

Table 2.1. Pressure and shear wave speeds and elastic properties of the glass layer (Publication II)

	h [mm]	ρ [kg/m ³]	c_p [m/s]	c_s [m/s]	G [GPa]	E [GPa]	ν
Float glass	7.88	2486±3	5914±39	3506±5	30.55±0.5	75.11±0.5	0.23±0.01
Tempered glass	7.92	2486±7	5852±58	3433±2	29.30±0.1	72.53±0.5	0.24±0.01

As it can be seen from Table 2.1, that the values of the wave speed and elastic parameters corresponding to the float and tempered glass are a quite close. Both, the pressure and shear wave speed are little higher (less than 3%) in the case of float glass. The Young and shear modulus are also higher in the case of the float glass (less than 5%). The value of the Poisson ratio is higher in the case of tempered glass (less than 5%).

Note, that in the case of glass the elastic properties depend on thickness on the glass sheet. Even more interesting – in the case of thin sheet the Young modulus is higher in the case of float glass and in the case of thicker sheets (over 10mm) the Young modulus is higher in the case of tempered glass. (Costa et al., 2006).

2.1.2 Four-point bending test for measuring strength properties of the glass layer and laminate

In order to determine the bending strength of the glass layer the following standardised four-point bending experiments were prepared on an Instron (Figure 2.3). The same test has been used for evaluating laminated glass panel.

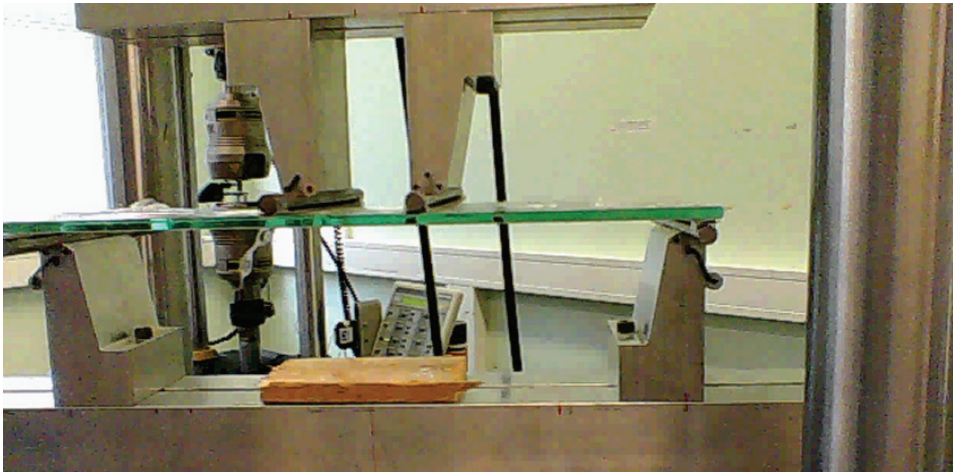


Figure 2.3. Setup of four-point bending test

The dimensions of the glass sheet used were (same for laminate): length 500 mm, width 200 mm, thickness 4mm/8mm. The distance between supporting rollers was 450mm and the distance between bending rollers 90mm. The bending strength is determined according to standard EN-ISO 1288-3 (Fors, 2014). In order to avoid excessive shattering, the specimens were wrapped into transparent film. The load speed 2 MPa/sec was used and the bending strength and the loading time up to failure is given in Table 2.2.

Table 2.2. Glass panel. The bending strength and the loading time up to failure

	Glass type	Actual thickness [mm]	Bending strength [kN]	Time at max load [sec]
1	Float glass	3.85	0.24	20
2	Float glass	3.86	0.25	21.1
3	Float glass	7.89	1.45	30.5
4	Float glass	7.89	1.3	27.3
5	Float glass	7.88	1.48	30.8
6	Tempered glass	7.91	3.81	79.4
7	Tempered glass	7.88	3.51	73.1

In the first two data rows and next three data rows of the Table 2.2 are given float glass panels with approximate thickness 4mm and 8 mm, respectively (exact thickness of each panel is shown in column 2). As it can be observed from Table 2.2, increasing the thickness of the glass panel twice will result increase of the bending strength over five times and increase of the load time up to failure about 1.5 times. In the last two rows of the Table 2.2 are given measuring data for tempered glass panels. Comparing these data with the data of the float glass panel of the same thickness one can observed that both, the bending strength and the load time up to failure increase over two times. Note, that the results given in Table 2.2 are obtained for particular selected glass panel but give also general understanding on strength behaviour of float and tempered glass panels. The location of the failure was in centre of the plate except second specimen when failure occurs at bending roller. The same setup has been used for evaluation of the laminated glass composite panels with the same geometry. Corresponding results are presented in Table 2.3.

Table 2.3. Laminated glass composite panel. The bending strength and the loading time up to failure

	Actual thickness [mm]	Bending strength [kN]	Time at max load [sec]
Laminate with float glass and PVB	8.42	0.91	19
Laminate with float glass and acoustic film	8.50	0.67	14.1
Laminate with tempered glass and PVB	8.39	2.7	56.9
Laminate with tempered glass and acoustic film	8.49	2.58	54.3

It can be observed from Table 2.3, that the bending strength of the laminates with PVB interlayer outperform that of the laminates with acoustic film interlayer. However, the differences of the bending strength are not drastical and the acoustic interlayer has obviously extra goal- to improved acoustic characteristics of the panel. Using tempered glass in laminate provide increase of bending strength near three times. For this reason, the tempered glass is widely used in laminates.

2.2 Interlayer

Standardised tensile tests were carried out to determine the stiffness and tensile strength properties of the interlayer. The testing apparatus was Instron Series 5800 electromechanical test system. The testing specimen type 5 was chosen according to ISO 527-3 (Figure 2.4).

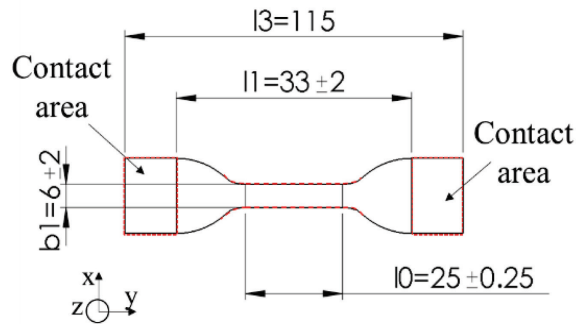


Figure 2.4. Specimen geometry

The tests were performed according to ISO-527-1 (Chen et al., 2016) and ISO-527-3 (Molnar et al., 2012) at room temperature at three different speeds: 500, 200 and 10 mm/min. Young's Modulus was determined at strain range between 0,0005 and 0,0025. The tensile strength was determined by breaking of the specimen, the corresponding values of the stress and strain were evaluated. The stress-strain relationship for different speed-rates is depicted on Figure 2.5.

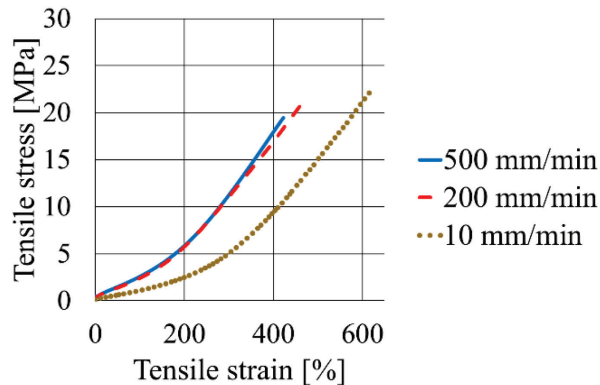


Figure 2.5. Tensile stress-strain graph (untreated PVB 0,76 mm)

From three to five repetitive tests were performed for each dataset and obtained results are given in Table 2.4.

Table 2.4. Stiffness and strength characteristics of 0,76 mm thick PVB interlayers

Speed rate [mm/min]	Young's Modulus [MPa]			
	PVB	Acoustic PVB	Heat treated PVB	Heat treated acoustic PVB
500	2,42±0,11	2,67±0,05	2,16±0,11	2,52±0,07
200	1,56±0,07	1,97±0,05	[-]	[-]
10	0,97±0,08	0,99±0,02	0,75±0,03	0,85±0,04
Tensile stress at break [MPa]				
500	23,89±0,03	20,33±0,05	22,15±0,10	17,96±0,12
200	24,03±0,06	20,56±0,06	[-]	[-]
10	21,34±0,09	15,63±0,08	19,70±0,04	14,77±0,01
Tensile strain at break [%]				
500	488,05±0,05	425,86±0,04	444,36±0,07	394,74±0,07
200	518,55±0,05	453,90±0,05	[-]	[-]
10	588,76±0,04	555,68±0,05	607,32±0,02	519,52±0,01

Following trends in regard on stiffness and strength can be observed:

- The heat treatment reduces the stiffness of standard PVB;
- The heat treatment reduces the stiffness of acoustic PVB;
- Using acoustic PVB will reduce the strength of the material;
- The heat treatment reduces the strength of standard PVB;
- The heat treatment reduces the strength of acoustic PVB.

Both stiffness and strength properties were time-dependant caused by visco-elastic material behaviour. Acoustic PVB appears most sensitive respect to speed rate.

Comparing the effect of heat treatment with using acoustic interlayer on can conclude that:

- Stiffness properties are more impacted by heat treatment;
- Strength properties are more impacted by utilising acoustic interlayer.

The conclusions made are valid for particular materials and dataset used above.

2.3 Residual stresses in glass

The testing of residual stress in annealed and tempered soda-lime glass was performed by private company GlasStress Ltd. The test equipment exploited for testing was scattered light polariscope SCALP-05. Figure 2.6. Specimens 500x200 mm with different thicknesses were measured from both tin and air side through the half of the thickness with small overlap. The tin side was ascertained with Tin Side Detector UV1301. Three different thickness specimens of tempered glass were tested: 4 mm, 8 mm and 4+4 mm laminated glass with 0,38 mm PVB interlayer. The setup of the measuring procedure is shown on Figure 2.6.

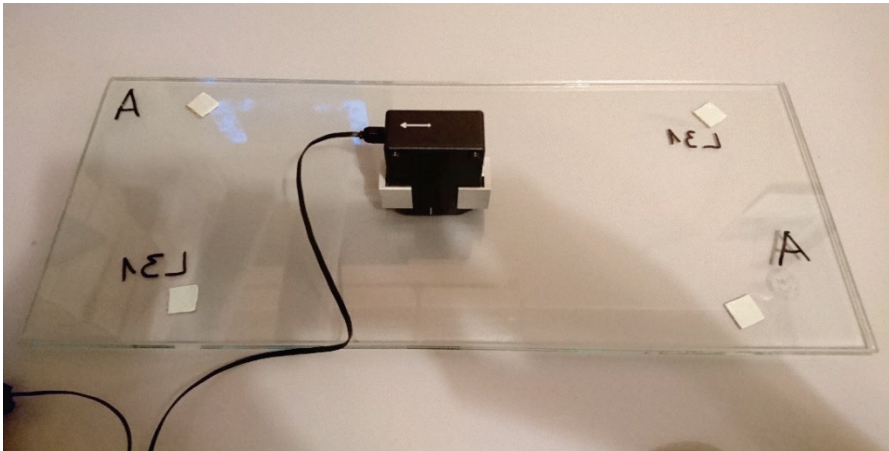


Figure 2.6. Measuring of the glass specimen with SCALP-05

Each specimen was measured along the direction of short (200 mm) and long (500 mm) side from ten different locations and the stress components σ_1 and σ_2 were obtained. The testing was performed with 0,01 mm step through the thickness. The results from tin and air side were combined into one curve (Figure 2.7).

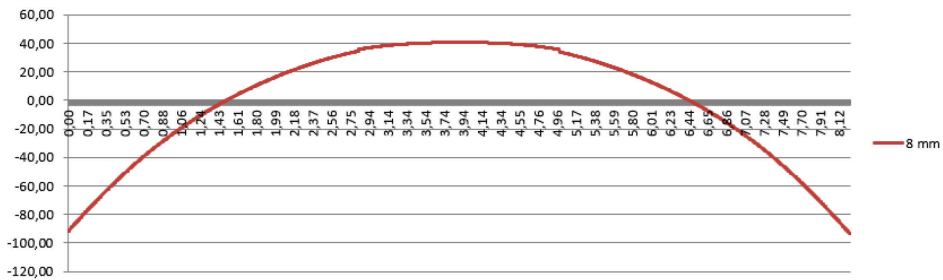


Figure 2.7. Stress component σ_1 distribution through the thickness for 8 mm tempered glass specimen (normal stress on vertical axis and specimen thickness on horizontal axis)

First were measured the through-the-thickness residual stresses in float glass from air side (Figure 2.8) and tin side (Figure 2.9). Here air side is a free upper side of the glass during manufacturing process and tin side is opposite side (in contact). The stresses are measured from both sides (air and tin) up to middle surface with small reserves. The red and blue lines stand for stress components σ_1 and σ_2 , respectively. Note that these components are just stresses along long and short side of the laminated glass specimen and not necessarily principal stresses. The stresses are negative (compression) near surfaces and positive (tension) near middle surface. Also, in the case of float glass the residual stresses remain small (less than 5 MPa).

Obviously, the values of the residual stresses are significantly higher. The surface stresses achieve the values $\sigma_1 = -89.4$ MPa, on $\sigma_2 = -89.9$ MPa on tin side and $\sigma_1 = -88$ MPa, on $\sigma_2 = -89.1$ MPa on air side. Similarly, to float glass the compression and tension stresses are observed near surface and middle surface, respectively. In figures 2.8 and 2.9 the through-the-thickness residual stress distribution is given for tempered laminated glass. The marking is conditional due to the lamination technology

where the glasses can be joined with both glasses facing air sides outward and both with tin side facing outward.

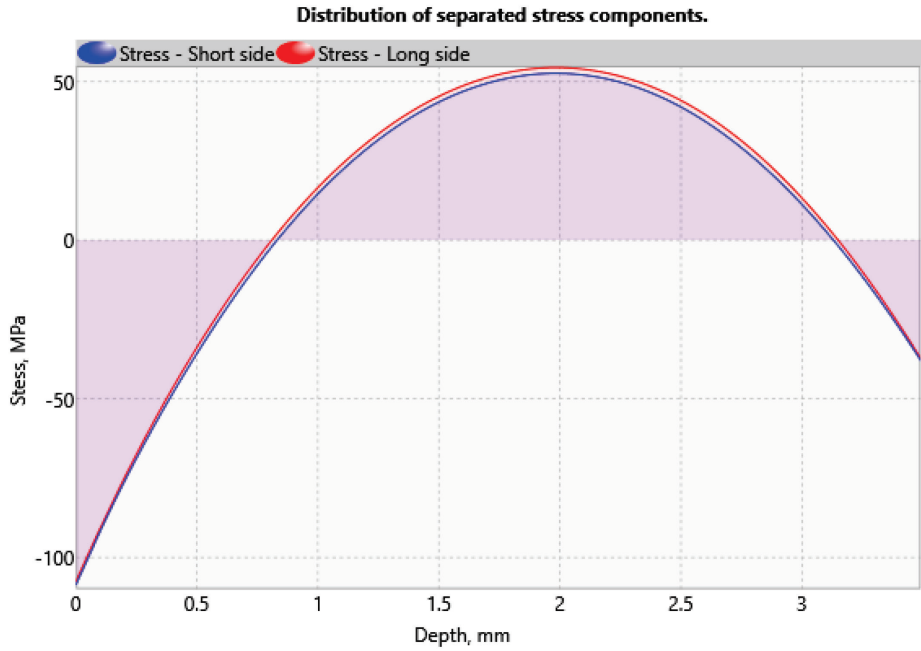


Figure 2.8. Stresses measured from the air side

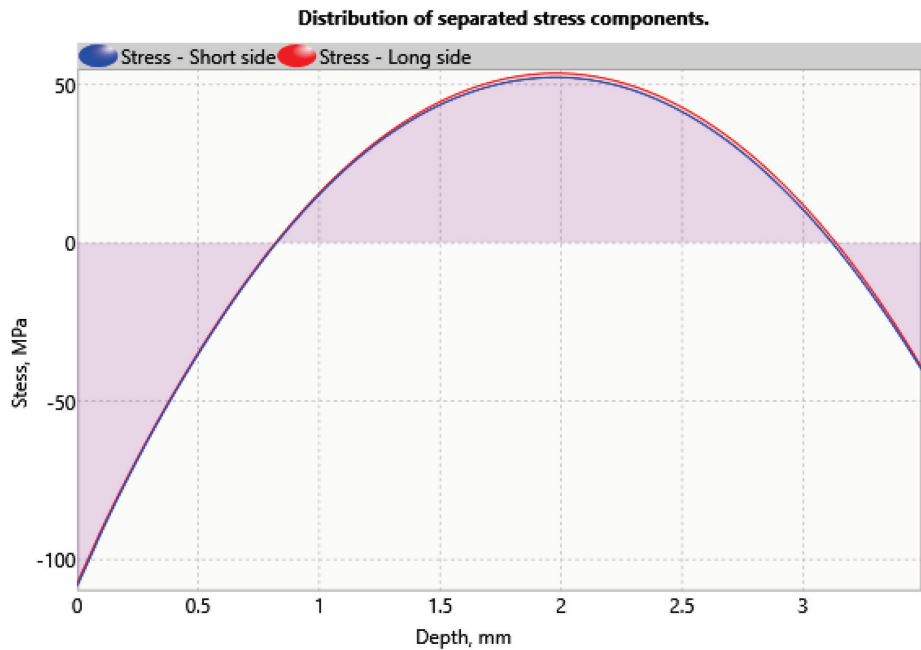


Figure 2.9. Stresses measured from the tin side

The average values of the stresses, corresponding to different glass sheets and laminates, are given in Table 2.5.

Table 2.5. Samples and average stress

Sample	Total sample thickness [mm]	Average stress in Tin side [MPa]	Average stress in AIR side [MPa]
Float glass sheet (4)	3,85	-2,90	-3,40
Float glass sheet (4)	3,86	-3,60	-3,30
Float glass sheet (4)	3,85	-1,80	-2,10
Float glass sheet (8)	7,89	-3,20	-3,30
Float glass sheet (8)	7,89	-3,20	-3,30
Float glass sheet (8)	7,88	-3,40	-3,20
Float glass sheet (8)	7,88	-3,60	-3,70
Tempered glass sheet (8)	7,91	-89,10	-89,10
Tempered glass sheet (8)	7,88	-89,60	-87,90
Laminate with float glass and PVB (4+h_inter+4)	8,42	-2,30	-3,00
Laminate with tempered glass and PVB (4+h_inter+4)	83,39	-101,80	-108,60
Laminate with float glass and acoustic film (4+h_inter+4)	8,50	-2,30	-2,60
Laminate with tempered glass and acoustic film (4+h_inter+4)	8,49	-106,70	-109,20

As it can be expected, the highest values of the residual stresses were measured in the case of tempered glass and laminated glass with tempered glass layers. The impact of the interlayer type (PVB or acoustic film) on values of the residual stresses is not significant.

3 Numerical modelling

In the following two case studies are considered: the design optimisation of the glass canopy panel and modelling residual stresses in glass panel.

3.1 Design of glass canopy panel

The work group has long time experience in area of design optimisation of various composite and sheet metal structures (Majak et al., 2017; Majak & Pohlak 2010; Kers et al., 2010; Pohlak et al., 2010; Karjust et al., 2010; Majak & Pohlak, 2010). Herein these techniques are adapted for design of glass structures. To analyse glass panel with point fixings, a three-dimensional FEM model is applied. The deformation of the glass canopy panel subjected to snow load may exceed the thickness of the panel (Figure 3.1).

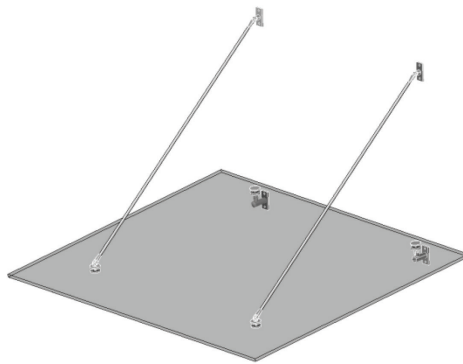


Figure 3.1 Glass canopy with point supports

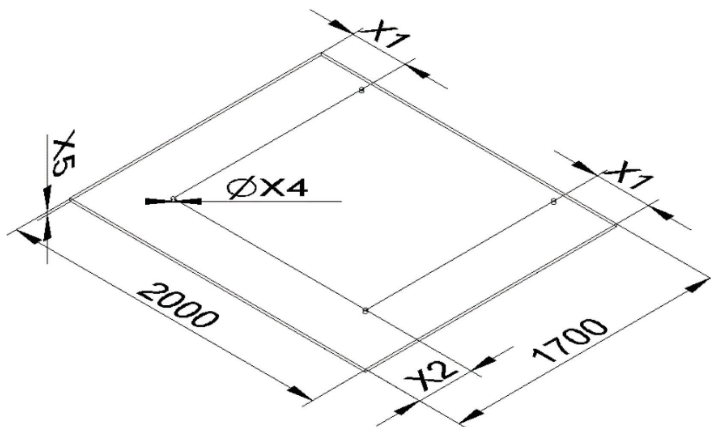


Figure 3.2. Design variables

Thereby the behaviour of the panel cannot be described accurately by linear theory. A nonlinear plate theory is applied. The stress-strain state of the glass panel is analysed

with FEA software (ANSYS) where simulation model with solid elements has been developed. For avoiding long calculation times, the general mesh element size of the model is delimited with 20 mm. Due to fact the maximum stresses occur around the fixing holes, the size of mesh elements around the holes is decreased to 3 mm. Such mesh is employed around holes in 40 mm diameter sphere.

The values of the design variables (Figure 3.2) are chosen based on manufacturing and structural limits. Four levels have been considered for the design variables X1, X2, X4 and three levels for X5, respectively. The value of the variable X3 is fixed due to technological limitations by the fixing manufacturer. Parametrical model according to the values of design variables was created in ANSYS Workbench. The maximum stresses occur on the edges of fixing holes (Figure 3.3).

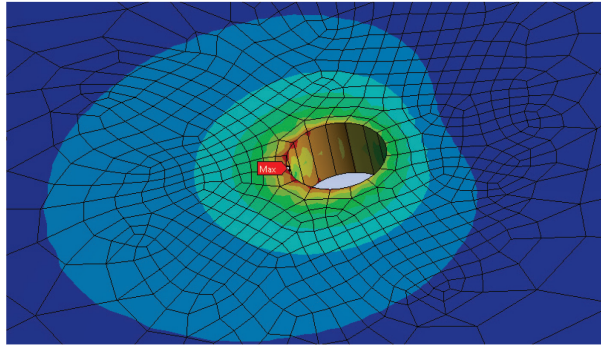


Figure 3.3. Stresses around fixing holes

In the following, the output data obtained from FE analysis are treated as response values. However, the evaluation of the objective functions by means FE simulations is time consuming. A common technique for reducing computational cost in optimization algorithms is using surrogate models for approximation of the objective functions.

In the current study the artificial neural networks (ANN) based surrogate models are employed to guide the search towards a global optimum. The Marquardt-Levenberg algorithm has been applied for training of a two-layer backpropagation artificial neural network. This algorithm combines the advantages of the steepest descent (wider convergence domain) and Newton (higher convergence speed) methods. The configuration of the ANN has been tuned for particular problem. The radbas neurons and purelin neurons are used in first and second network layers, respectively.

At starting point the number of neurons is selected as (Gnana Sheela & Deepa, 2013)

$$N_h = \frac{(N_{in} + \sqrt{N_{tr}})}{L}, \quad (3.1)$$

and the number of neurons is increased by one up to ANN model error is decreasing. In (3.1) N_{in} and N_{tr} stand for number of inputs and the capacity of the training data, respectively. The default value of the learning rate 0.05 has been employed.

The considered optimisation problem is a mixed integer problem. The design variables X1 and X2, describing positions of the holes are real valued, but the radius of the hole and thickness have integer values. An analysis of the optimality criteria has been performed and different formulations of the optimisation problem are examined.

The minimisation of the maximum value of the Von Mises stress and maximum deflection are considered as two criteria

$$f_1(\bar{x}) = \min(\sigma_{max}^{VonMises}), \quad (3.2)$$

$$f_2(\bar{x}) = \min(\varepsilon_{max}), \quad (3.3)$$

subjected to

$$x_{i*} \leq x_i \leq x_i^*; \quad i = 1, \dots, n, \quad (3.4)$$

$$\varepsilon_{max}(\bar{x}) \leq \varepsilon_{max}^*(\bar{x}), \quad (3.5)$$

$$C(\bar{x}) \leq C^*(\bar{x}). \quad (3.6)$$

Table 3.1. Objective functions and optimal solutions

Objective	X1	X2	X4	X5
f_1	394.56	450.00	35	20
f_2	399.51	450.00	34	20
f_3	396.52	450.00	35	20

The objective $f_3(\bar{x})$ shown in last row of the Table 3.1 is defined as weighted sum of the objectives $f_1(\bar{x})$ and $f_2(\bar{x})$ as

$$f_3(\bar{x}) = w_1 f_1(\bar{x}) + w_2 f_2(\bar{x}). \quad (3.7)$$

Here the weights w_1 and w_2 determine the significance of the corresponding criteria

$$w_1 + w_2 = 1. \quad (3.8)$$

In Table 3.1 the values of the design variables are given in original dimensions in order to simplify understanding their real meaning.

The hybrid genetic algorithm (HGA) is adapted for solving above considered mixed integer optimisation problem (Zhang et al., 1999; Guessasma et al., 2015; Zhu et al., 2018).

As it can be expected the two criteria: minimisation of the maximum Von Mises stress and maximum deformations are not conflicting. Thus, the use of weighted summation techniques for combining these criteria is justified. Employing the weighted summation criterion (3.7) allows to consider two objectives but perform optimisation with one combined objective. The weights w_1 and w_2 can be assigned according to significance of the objectives (higher weight to more critical objective).

It can be seen from Figure 3.1 that the values of the design variables corresponding to combined objective remains between the values of the single objectives (X1) or coincide with these values. Also, the optimal solutions corresponding to different criteria are close.

The values of the thickness (X5) are equal to upper limit since the cost is not considered as objective function and constraints on value of the cost (4) applied appears satisfied in the case of all optimal designs considered (in general increasing thickness improve mechanical performance but increase cost).

Next, the cost is considered as third objective. The cost has been observed to be conflicting criteria for both above considered criteria and their weighted sum (Figure 3.4)

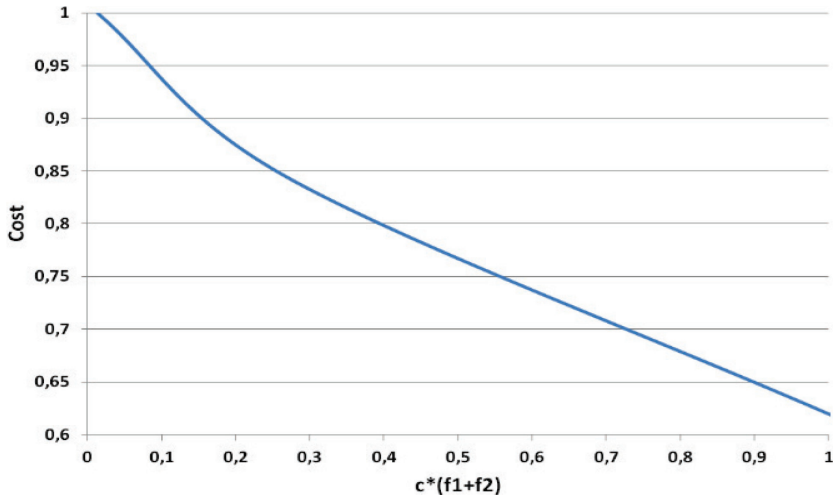


Figure 3.4. Pareto front. Cost vs. combined mechanical characteristics

Each point in Pareto front is optimal solution i.e. best available results for particular given cost. Moving on Pareto front from right to left, we improve the values of the mechanical characteristics (maximum stress and strain values decrease), but the value of the cost is increasing at the same time (Figure 3.4). Obviously, the Pareto front provide much more information in comparison with weighted summation etc. techniques. However, certain consideration is necessary for selection of the final optimal solution (it can be made based on cost or some additional information).

3.2 Modelling residual stresses in glass panel

This chapter cover determination of the residual stresses and their incorporation in FEM models.

3.2.1 Determination residual shear stresses in glass

The shear stresses σ_{12} in glass panel can be determined based on measured values of normal stresses by applying the plane stress tensor rotation formulas. For this reason, the following procedure is proposed:

- The initial coordinate system was specified by long and short sides of the glass specimen;
- The stress components $\sigma_1^{\text{exp}_0}$ and $\sigma_2^{\text{exp}_0}$ were measured in initial coordinate system;
- The stress components $\sigma_1^{\text{exp}_\theta}$ and $\sigma_2^{\text{exp}_\theta}$ were measured in coordinate system rotated by angle θ° ;
- By applying the plane stress tensor rotation formulas, the expected theoretical values of the stress components $\sigma_1^{\text{theoret}_\theta}$ and $\sigma_2^{\text{theoret}_\theta}$ can be computed as

Again, since the value of the shear stress σ_{12}^0 is unknown, the formulas (3.14) are not directly applicable. Similarly, to the done above, the shear stress σ_{12}^0 can be considered as design variable and determined as solution of the following optimisation problem

$$f = \left(\sigma_1^{\text{theoret}\theta_1} - \sigma_1^{\text{exp}\theta_1} \right)^2 + \left(\sigma_2^{\text{theoret}\theta_1} - \sigma_2^{\text{exp}\theta_1} \right)^2 + \dots \\ + \left(\sigma_1^{\text{theoret}\theta_n} - \sigma_1^{\text{exp}\theta_n} \right)^2 + \left(\sigma_2^{\text{theoret}\theta_n} - \sigma_2^{\text{exp}\theta_n} \right)^2 \rightarrow \min. \quad (3.15)$$

Applying the stationary condition (3.12) for function (3.15) and considering that the experimentally measured values of stresses are given constants one obtains

$$\frac{\partial f}{\partial \sigma_{12}^0} = 2 \left(\sigma_1^{\text{theoret}\theta_1} - \sigma_1^{\text{exp}\theta_1} \right) \frac{\partial \sigma_1^{\text{theoret}\theta_1}}{\partial \sigma_{12}^0} + 2 \left(\sigma_2^{\text{theoret}\theta_1} - \sigma_2^{\text{exp}\theta_1} \right) \frac{\partial \sigma_2^{\text{theoret}\theta_1}}{\partial \sigma_{12}^0} + 2 \left(\sigma_1^{\text{theoret}\theta_n} - \sigma_1^{\text{exp}\theta_n} \right) \frac{\partial \sigma_1^{\text{theoret}\theta_n}}{\partial \sigma_{12}^0} + 2 \left(\sigma_2^{\text{theoret}\theta_n} - \sigma_2^{\text{exp}\theta_n} \right) \frac{\partial \sigma_2^{\text{theoret}\theta_n}}{\partial \sigma_{12}^0} = 0 \quad (3.16)$$

In (3.16) the derivatives can be computed based on formulas (3.14) as

$$\begin{cases} \frac{\partial \sigma_1^{\text{theoret}\theta_1}}{\partial \sigma_{12}^0} = 2 \sin(\theta_1) \cos(\theta_1), \dots, \frac{\partial \sigma_1^{\text{theoret}\theta_n}}{\partial \sigma_{12}^0} = 2 \sin(\theta_n) \cos(\theta_n) \\ \frac{\partial \sigma_2^{\text{theoret}\theta_1}}{\partial \sigma_{12}^0} = -2 \sin(\theta_1) \cos(\theta_1), \dots, \frac{\partial \sigma_2^{\text{theoret}\theta_n}}{\partial \sigma_{12}^0} = -2 \sin(\theta_n) \cos(\theta_n) \end{cases}. \quad (3.17)$$

The equation (3.16) can be reorganised as

$$2[\sin^2(2\theta_1) + \dots + \sin^2(2\theta_n)]\sigma_{12}^0 + [\sin(2\theta_1) \cos(2\theta_1) + \dots + \sin(2\theta_n) \cos(2\theta_n)] \left(\sigma_1^{\text{exp}\theta_1} - \sigma_2^{\text{exp}\theta_1} \right) + [\sin(2\theta_1) \left(\sigma_2^{\text{exp}\theta_1} - \sigma_1^{\text{exp}\theta_1} \right) + \dots + \sin(2\theta_n) \left(\sigma_2^{\text{exp}\theta_n} - \sigma_1^{\text{exp}\theta_n} \right)] = 0 \quad (3.18)$$

The equation (3.18) is linear with respect to design variable σ_{12}^0 , and its unique solution can be given as

$$\sigma_{12}^0 = \frac{[\sin(2\theta_1) \cos(2\theta_1) + \dots + \sin(2\theta_n) \cos(2\theta_n)] \left(\sigma_1^{\text{exp}\theta_1} - \sigma_2^{\text{exp}\theta_1} \right) + \text{sum}_n}{2[\sin^2(2\theta_1) + \dots + \sin^2(2\theta_n)]}, \quad (3.19)$$

where

$$\begin{aligned} sum_n = & \sin(2\theta_1) \left(\sigma_2^{\text{exp}\theta_1} - \sigma_1^{\text{exp}\theta_1} \right) + \dots \\ & + \sin(2\theta_n) \left(\sigma_2^{\text{exp}\theta_n} - \sigma_1^{\text{exp}\theta_n} \right). \end{aligned} \quad (3.20)$$

It can be confirmed, that in the special case where $n = 1$ the formulas (3.19)–(3.20) reduces to (3.13). It is correct to point out that the cost needed to pay for higher accuracy is higher number of experiments (the normal stresses should be measured for each value of $\theta_i, i = 1, \dots, n$).

3.2.2 Error estimation algorithm for residual normal stresses

The error can be estimated based on the measured values of the normal stresses $\sigma_1^{\text{exp}-0}, \sigma_2^{\text{exp}-0}$ in initial coordinate system and computed shear stress σ_{12}^0 . Utilising the stress tensor rotation formulas, the theoretical values of normal stresses $\sigma_1^{\text{theoret}_\theta}$ and $\sigma_2^{\text{theoret}_\theta}$ can be computed. The errors of the measured normal stresses can be expressed as

$$e_1 = \left| \sigma_1^{\text{exp}\theta} - \sigma_1^{\text{theoret}_\theta} \right|, \quad (3.21)$$

$$e_2 = \left| \sigma_2^{\text{exp}\theta} - \sigma_2^{\text{theoret}_\theta} \right|, \quad (3.22)$$

Obviously both measurements at angle 0 and θ degrees have impact on computed errors. In the case of biggest values of the stresses, occurring near outer surfaces, the error of residual stresses was estimated near 1%.

3.2.3 Incorporating residual stresses in FEM model

The stress components obtained from the testing and the calculated shear stress components can be incorporated into user defined FE model. However, much simpler approach, introduced below, is also available (also more robust).

Incorporating residual stresses in FEM model through resultant forces

First note, that based on results of measurements and evaluated shear stresses, the following assumptions can be made for simplified model:

- The shear stresses can be omitted (relatively small in the case of considered problem, approximately 70 times smaller than the normal stresses),
- The stress distribution is assumed constant in plane of glass panel (x, y directions)

The normal stress distribution over the cross-section can be approximated by the resultant forces computed as

$$F_x = \int_A \sigma_x dA = b * \int_{-\frac{h}{2}}^{\frac{h}{2}} \sigma_x dz; \quad F_y = \int_A \sigma_y dA = L * \int_{-\frac{h}{2}}^{\frac{h}{2}} \sigma_y dz. \quad (3.23)$$

In (3.23) A is a cross-section area, L and b are length and width of the glass sheet. The σ_x and σ_y stand for the normal stresses in longitudinal and transverse directions, respectively. The resultants forces in longitudinal and transverse directions are denoted

by F_x and F_y , respectively. For measured values of the normal stresses σ_x and σ_y , the integrals included in (3.23) can be calculated by applying Simpson formulas in the following form

$$\int_{-h/2}^{h/2} \sigma_x dz = \frac{h}{3} \left[\sigma_x(z_0) + 4\sigma_x(z_1) + 2\sigma_x(z_2) + 4\sigma_x(z_3) + \dots + 2\sigma_x(z_{n-1}) + \sigma_x(z_n) \right], \quad (3.24)$$

$$\int_{-h/2}^{h/2} \sigma_y dz = \frac{h}{3} \left[\sigma_y(z_0) + 4\sigma_y(z_1) + 2\sigma_y(z_2) + 4\sigma_y(z_3) + \dots + 2\sigma_y(z_{n-1}) + \sigma_y(z_n) \right], \quad (3.25)$$

where

$$z_i = -\frac{h}{2} + i * \frac{h}{n}, \quad (3.26)$$

and n stands for the number of equally spaced subdivisions (n is even number).

The resultant forces F_x and F_y evaluated using (3.23) can be utilised in user defined FEM model. Obviously, the calculated values of the resultant forces may correspond for wide class of different stress distributions and thus the proposed approach can be considered as simplified approximation. Note, that the resultants moments caused by residual stresses appear several magnitudes less than resultant forces considered and were omitted in simplified model proposed.

The mesh of the model includes eight layers through the thickness. In other directions the mesh is divided into 100 elements (Figure 3.4).

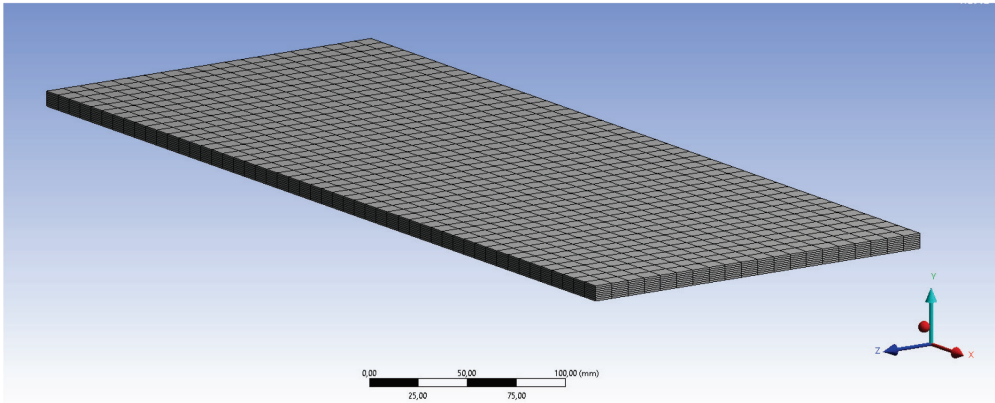


Figure 3.4. FE mesh for modal analysis of the glass panel

The calculated resultant forces are applied on a glass panel fixed as a console (Figure 3.5). In the Table 3.2 are presented the results of modal analysis of non-stressed and prestressed glass panel.

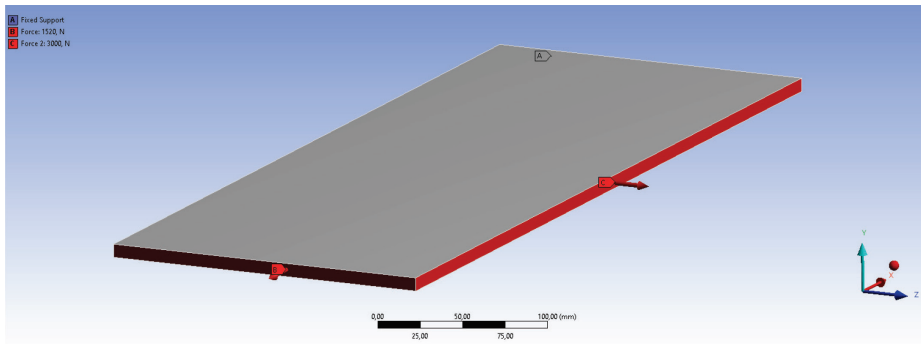


Figure 3.5. The application of the resultant forces

Table 3.2. Comparison between prestressed and non-stressed glass

Mode nr	Without prestress Frequency [Hz]	Prestressed with resultant forces Frequency [Hz]
1	28,9	31,4
2	154,4	155,1
3	180,6	181,4

It can be concluded that the prestressed state elevates the natural frequencies of the body although the effect is not very remarkable.

Incorporating residual stresses in FEM by direct insertion in nodes

The measured prestresses σ_x and σ_y and the calculated shear stress σ_{xy} are applied onto the element corner nodes of the FEM model. The mesh sizing is the same as in the previous step with resultant forces. The stress is applied on 9639 points (Figure 3.6).

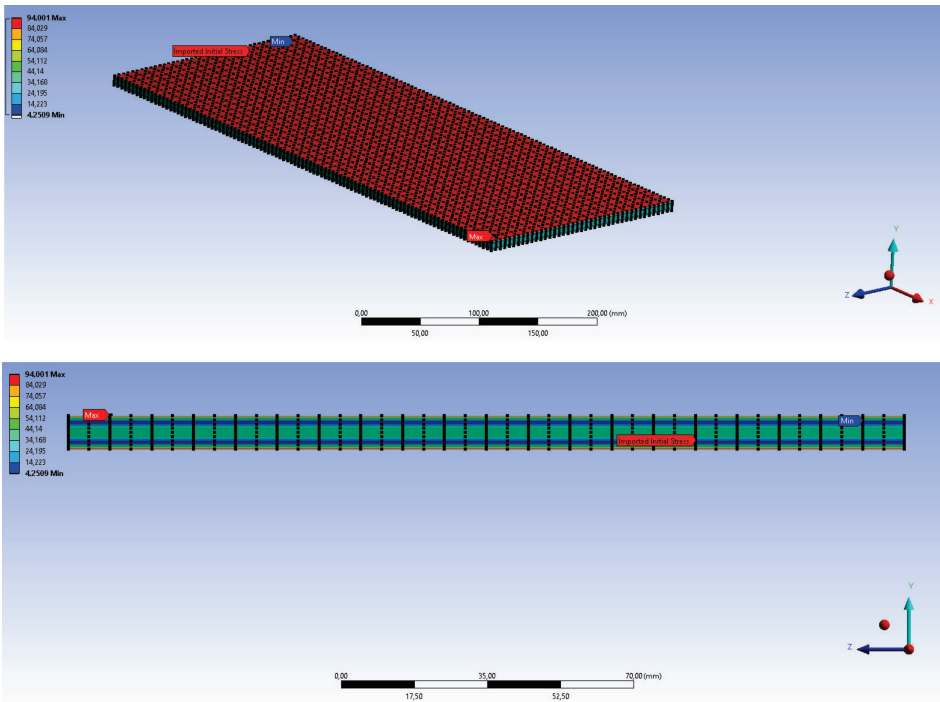


Figure 3.6. Applied initial stress

The results of the direct inserted residual stress model are presented in the Table 3.3.

Table 3.3. Modal results for direct insertion model

Mode nr	Frequency [Hz]
1	28,5
2	151,2
3	177,4

From the direct incorporation can be deduced that the method will result in lower frequencies than non-prestressed model and robust model. The effect is caused by two aspects:

- 1) The elastic modulus and Poisson's ratio for tempered (prestressed) glass are expected to be lower than for float glass (Table 2.1; Costa et al., 2006), Table 2.1. Pressure and shear wave speeds and elastic properties of the glass layer (Publication II)
- 2) Due to the console fixation the specimen is free to stress relaxation.

From two models proposed for incorporation residual stresses the first can be considered as preliminary robust model.

4 Conclusion

According to the main goal of the study, the methodology for an accurate analysis and design of glass panels and laminated glass composite panels has been developed. An approach proposed is based on combining experimental study, theoretical and numerical analysis.

Experimental study:

First the experimental evaluation of the mechanical properties of glass panel or layers of the glass laminate panel is performed. The measuring of the normal components of the residual stresses is included. The mechanical properties of glass (glass layers) are determined by use of non-destructive testing. The longitudinal pressure wave (P-wave) and shear wave (S-wave) wave speed is determined and based on obtained results the elasticity parameters are computed (Young's modulus and Poisson ratio). The mechanical properties of the interlayer are determined from traditional tension tests due material properties and small thickness.

Theoretical analysis:

By applying optimisation methods and rotation formulas of the plane stress tensor, the algorithm for determining the value of the shear stress component is developed. The error estimation algorithm for measured normal components of the residual stresses is developed based on the same approach. A simplified approach has been developed for incorporating the measured residual stresses in FEM model. Particularly, the residual stresses through thickness of the glass sheet are replaced by corresponding resultant forces and moments.

Numerical analysis:

Several FEM models are developed for analysis and design of glass panels. In the case of glass canopy panel, the FEM results are used for artificial neural network based response modelling and further design optimisation. The FEM model, involving the measured residual stresses, has been introduced.

Based on the experimental study, theoretical and numerical analysis performed, the following conclusions can be made for the activities introduced in section 1.4:

Activity 1:

The stiffness properties of the glass panel/layer have been determined from non-destructive tests, based on measuring longitudinal pressure wave (P-wave) and shear wave (S-wave) wave speed. The elastic modulus of the thermally treated glass is lower non-treated FG. The elastic modulus of the interlayer of laminate have been determined from traditional tensile tests.

Activity 2:

Design of experiment for measuring residual stresses has been developed. The measurements are performed using different rotation angle. This allow to determine the shear stress component from optimisation procedure proposed.

Activity 3:

Two approaches for integration residual stresses in FEM model are proposed. Robust method with resultant forces and direct application of measured normal stresses onto FE nodes are introduced. FEM simulation model for analysis of glass structures including effect of residual stresses was introduced

Activity 4:

GA and hybrid GA algorithms are combined with ANN and FEM analysis results for design optimisation glass canopy panel.

Obviously, the conclusions made, based on activities, cover the activities and the hypotheses given in section 1.5.

The Scientific Novelty

The scientific novelties of the study can be outlined as:

- An approach, based on combining experimental study, theoretical and numerical analysis for design and analysis of the glass structures, is proposed.
- The algorithm is developed for determining the shear stress component of the plane stress tensor.
- The error estimating algorithm has been developed for of the experimentally measured residual normal stresses.
- Two approaches have been proposed for integration residual stresses in FEM model.

Future work

The future study is related with further improvement of the FEM model incorporation the residual stresses. Challenging topic is utilising new material models for interlayer, evaluation acoustic properties of the interlayers and glass laminate panel, etc.

References

Achintha, M. (2016). *Sustainability of Construction Materials (2nd ed.)*. Cambridge, GB: Woodhead Publishing.

Arram, A., Ayob, A. (2019). A novel multi-parent order crossover in genetic algorithm for combinatorial optimization problems. *Computers & Industrial Engineering, Volume 133*, 267–274.

Aruniit, A., Kers, J., Goljandin, D., Saarna, M., Tall, K., Majak, J., Herranen, H. (2011). Particulate Filled Composite Plastic Materials from Recycled Glass Fibre Reinforced Plastics. *Materials Science (Medžiagotyra)*, 17, 276–281.

Askeland, D.R., Fulay, P.P., Wright, W.J. (2010). *The Science and Engineering of Materials (6th ed.)*. Cengage Learning.

Auriemma, F. (2017). A double-layer acoustic absorber as potential substitute for traditional micro-perforated elements. *Proceedings of Meetings on Acoustics Meeting of Acoustic Society of America*, 30.

Auriemma, F. (2017). Acoustic Performance of Micro-Grooved Elements. *Applied Acoustics*, 122, 128–137.

Auriemma, F. (2017). Study of a New Highly Absorptive Acoustic Element. *Acoustics Australia*, 45, 411–419.

Belegundu, A.D., Chandrupatla, T.R. (2012). *Optimization Concepts and Applications in Engineering (2nd ed.)*, New York, NY, USA: Cambridge University Press.

Brisset, S., Gillon, F. (2015). Approaches for multi-objective optimization in the ecodesign of electric systems. In: Bessedé, J.-L. (Ed.) *Eco-Friendly Innovation in Electricity Transmission and Distribution Networks*, 83–97. Cambridge, GB: Woodhead Publishing.

Chen, S., Zang, M., Wang, D., Zheng, Z., Zhao, C. (2016). Finite element modelling of impact damage in polyvinyl butyral laminated glass. *Composite Structures*, 138, 1–11.

Chong, E.K.P., Zak, S.H. (2013). *An Introduction to Optimization (4th ed.)*. New York, NY, USA: John Wiley & Sons.

Chunka, C., Goswami, R.S., Banerjee, S. (2018) An efficient mechanism to generate dynamic keys based on genetic algorithm. *Security and Privacy*, 37, 1–10.

Costa, S., Miranda, M., Varum, H., Teixeira-Dias, F. (2006). On the Evaluation of the Mechanical Behaviour of Structural Glass Elements. *Materials Science Forum*, 514-516, 799–803.

Deb, K. (2000). Introduction to representations. In T. Bäck, D.B. Fogel & T. Michalewicz (Ed.). *Evolutionary Computation 1: Basic Algorithms and Operators* (pp. 127-131). Bristol, UK: Institute of Physics Publishing.

Dorigo, M. (1992). *Optimization, Learning and Natural Algorithms*. PhD Thesis, Milan, Italy: Dipartimento di Elettronica, Politecnico di Milano.

Dupont (2019, October 11). *DuPont SentryGlas Architectural Safety Glass Interlayer*. Retrieved from <http://www.faglass.com/alliances-pdf/SentryGlas1.pdf>

Eisenträger, J., Naumenko, K., Altenbach, H., Köppe, H. (2015). Application of the first-order shear deformation theory to the analysis of laminated glasses and photovoltaic panels. *International Journal of Mechanical Sciences*, 96-97, 163–171.

- Ferreira, R.T.L., Rodrigues, H.C., Guedes, J.M., Hernandez, J.A. (2014). Hierarchical optimization of laminated fiber reinforced composites. *Composite Structures*, 107, 246–259.
- Fors, C. (2014). Mechanical Properties of Interlayers in Laminated Glass, Masters Dissertation, Lund, Sweden: Lund University.
- Fröling, M. (2013). *Strength Design Methods for Glass Structures*, Lund, Sweden: Lund University.
- Fröling, M. (2009). *Strength Design Methods for Laminated Glass*. Licentiate Dissertation, Lund, Sweden: Lund University.
- García-Martínez, C., Lozano, M. (2007). Local Search Based on Genetic Algorithms. In P. Siarry, Z. Michalewicz (Ed.). *Advances in Metaheuristics for Hard Optimization*, (199–221). New York, NY, USA: Springer.
- Glass Academy (2019, Nov 13). *Tempered Glass*. Retrieved from <http://www.glass-academy.com/tempered-glass-2/>
- Glover, F. (1990). Tabu search—Part 2. *ORSA Journal of Computing*, 2, 4–32.
- Gnana Sheela, K., Deepa, S.N. (2013). Review of Methods to Fix Number of Hidden Neurons in Neural Networks. *Mathematical Problems in Engineering*, 6.
- Guardian Glass. (2019, September 8). *What is the difference between heat-strengthened and fully tempered glass?* Retrieved from <https://www.guardianglass.com/us/en/tools-and-resources/library/faqs/commercial/heat-strengthened-and-fully-tempered>
- Guessasma, S., Bassir, D., Hedjazi, L. (2015). Influence of interphase properties on the effective behaviour of a starch-hemp composite. *Materials and Design*, 65, 1053–1063.
- Hajkowicz, S., Higgins A. (2008) A comparison of multiple criteria analysis techniques for water resource management. *Journal of Operational Research*, 184, 255–265.
- Herranen, H., Majak, J., Tsukrejev, P., Karjust, K., Märtens, O. Design and Manufacturing of composite laminates with structural health monitoring capabilities, *Procedia CIRP*, 72, 647–652.
- Herranen, H., Pabut, O., Eerme, M., Majak, J., Pohlak, M., Kers, J., Saarna, M., Allikas, G., Aruniit, A. (2011). Design and Testing of Sandwich Structures with Different Core Materials. *Journal of Materials Science of Kaunas University of Technology*, 17, 1–6.
- Holland, J.H. (1975). *Adaptation in Natural and Artificial Systems*. Ann Arbor, MI, USA: The University of Michigan Press.
- Iqbal, K. (2013). *Fundamental Engineering Optimization Methods (2nd ed.)*. Retrieved from <http://www.ist.edu.pk/downloads/cacss/workshops/national/optimum-engineering-design-workshop/fundamental-engineering-optimization-methods-2e.pdf>
- Javidrad, F., Nazari, M., Javidrad H.R. (2018). Optimum stacking sequence design of laminates using a hybrid PSO-SA method. *Composite Structures*, 185, 607–618.
- Jebari, K., Madiafi, M. (2013). Selection Methods for Genetic Algorithms. *International Journal of Emerging Sciences*, 3, 333–344.
- Karjust, K., Pohlak, M., Majak, J. (2010). Optimal adhesion measuring methods of the glass fiber reinforcement layer. *Estonian Journal of Engineering*, 16, 297–306.

- Keller, D. (2010). Optimization of ply angles in laminated composite structures by a hybrid, asynchronous, parallel evolutionary algorithm. *Composite Structures*, *92*, 2781–2790.
- Kennedy, J., Eberhart, R. (1995). Particle swarm optimization, *Proceedings of IEEE International Conference on Neural Networks*, *4*, 1942–1948, Perth, WA, Australia: IEEE.
- Kers, J., Majak, J., Goljandin, D., Gregor, A., Malmstein, M.; Vilsaar, K. (2010). Extremes of apparent and tap densities of recovered GFRP filler materials. *Composite Structures*, *92*, 2097–2101.
- Kuhn, H.W., Tucker, A.W. (1951) Nonlinear programming. In J. Neyman (Ed.). *Proceedings of Second Berkeley Symposium on Mathematical Statistics and Probability* (481–492). Oakland, CA, USA: University of California Press.
- Kurdi, M.H. (2005). *Robust Multi-criteria Optimization of Surface Location Error and Material Removal Rate in High-Speed Milling under uncertainty*. PhD Thesis, Gainesville, FL, USA: University of Florida.
- Lorraine F.F. (2016). *Materials Processing. A Unified Approach to Processing of Metals, Ceramics and Polymers*. Oxford, UK: Academic Print.
- Majak, J., Kirs, M., Eerme, M., Tungel, E., Lepikult, T. (2017). Design optimization of graphene laminates for maximum fundamental frequency. *Proceedings of the Estonian Academy of Sciences*, *66*, 354–362.
- Majak, J., Pohlak, M. (2010). Decomposition method for solving optimal material orientation problems. *Composite Structures*, *92*, 1839–1845.
- Majak, J., Pohlak, M. (2010). Optimal material orientation of linear and non-linear elastic 3D anisotropic materials. *Meccanica*, *45*, 671–680.
- Majak, J., Pohlak, M., Eerme, M., Velsker, T. (2012). Design of car frontal protection system using neural networks and genetic algorithm. *Mechanika*, *18*, 453–460.
- Marini, F., Walczak, B. (2015). Particle swarm optimization (PSO). A tutorial. *Chemometrics and Intelligent Laboratory Systems*, *149*, 153–165.
- Molnar, G., Vighi, L., Dunai, L. (2012). Finite element analysis of laminated structural glass plates with polyvinyl butyral (PVB) interlayer. *Periodica Polytechnica Civil Engineering*.
- Naumenko, K. Eremeyev, V. A. (2014). A layer-wise theory for laminated glass and photovoltaic panels. *Composite Structures*, *112*, 283–291.
- Nik, A.A., Nejad, F.M., Zakeri, H. (2016). Hybrid PSO and GA approach for optimizing surveyed asphalt pavement inspection units in massive network. *Automation in Construction*, *71*, 325–345.
- Nyounguè, A., Bouzid, S., Dossou, E., Azari, Z. (2016). Fracture characterisation of float glass under static and dynamic loading. *Journal of Asian Ceramic Societies*, *4*, 371–380.
- Pfaender, H.G. (1996). *Schott Guide to Glass*. Springer Netherlands.
- Pohlak, M., Majak, J., Karjust, K., Küttner, R. (2010). Multicriteria optimization of large composite parts. *Composite Structures*, *92*, 2146–2152.
- Quesada, A (2019, Oct 12). *5 algorithms to train a neural network*. Retrieved from https://www.neuraldesigner.com/blog/5_algorithms_to_train_a_neural_network

- Reguera, F., Cortínez, V.H. (2016). Optimal design of composite thin-walled beams using simulated annealing. *Thin-Walled Structures*, 104, 71–81.
- Şahman, M. A., Çunkaş, M., İnal, Ş., İnal, F., Coşkun, B. and Taşkıran, U. (2009) Cost optimization of feed mixes by genetic algorithms. *Advances in Engineering Software*, 40, 965–974.
- Santosa, B. (2019, Nov 8). *Tutorial on Ant Colony Optimization*. Retrieved from <https://bsantosa.files.wordpress.com/2015/03/aco-tutorial-english2.pdf>
- Serbena, F.C., Zanotto, E.D. (2012). Internal residual stresses in glass-ceramics: A review. *Journal of Non-Crystalline Solids*, 358, 975–984.
- Smith, J.C., Taşkın, Z.C. (2008). A Tutorial Guide to Mixed-Integer Programming Models and Solution Techniques. In G. J. Lim and E. K. Lee (Ed.). *Optimization in Medicine and Biology*. Boca Raton, FL, USA: Auerbach Publications.
- Storn, R., Price, K. (1997). Differential evolution – a simple and efficient heuristic for global optimization over continuous spaces. *Journal of Global Optimization*, 11, 341–359.
- Vaissier, B., Pernot, J.-P., Chougrani, L., Véron, P. (2019) Genetic-algorithm based framework for lattice support structure optimization in additive manufacturing. *Computer-Aided Design*, 110, 11–23.
- Vosoughi, R., Gerist, S. (2014). New hybrid FE-PSO-CGAs sensitivity base technique for damage detection of laminated composite beams. *Composite Structures*, 118, 68–73.
- Wang, Z., Wang, Y., Liang, Y., Du, X., Shi, Y. (2016). Bearing capacity of tempered glass panel in point supported glass facades against in-plane load. *Archives of Civil and Mechanical Engineering* (16), 935–948.
- Yan, L., Shuxia, R. (2011). *Building Decorative Materials*. Cambridge, GB: Woodhead Publishing.
- Zhang, W.H., Domaszewski, M., Bassir, D. (1999). Developments of sizing sensitivity analysis with the ABAQUS code. *Structural Optimization*, 17, 219–225.
- Zhang, X., Hao, H. (2015). *Construction and Building Materials* (93rd ed.), 404–415.
- Zhu, J., Zhang, W., Xia, L., Zhang, Q., Bassir, D. (2018). Optimal packing configuration design with finite-circle method. *Journal of Intelligent and Robotic Systems: Theory and Applications*. 67, 185–199.
- Zitzler, E., Thiele, L. (1999). Multiobjective evolutionary algorithms: A comparative case study and the strength Pareto approach. *IEEE Transactions on Evolutionary Computation*, 3, 257–271.

Acknowledgements

I would like to thank my supervisors prof. Jüri Majak and prof. Martin Eerme for the guidance, encouragement and motivation I am thankful to all the coauthors who contributed to the publications associated to the thesis.

The research was supported by the Estonian Research Council (grant PUT1300); Estonian Centre of Excellence in Zero Energy and Resource Efficient Smart Buildings and Districts, ZEBE, TK146 funded by the European Regional Development Fund (grant 2014-2020.4.01.15-0016); Innovative Manufacturing Engineering Systems Competence Centre IMECC (supported by Enterprise Estonia and co-financed by the European Union Regional Development Fund, project EU48685).

Abstract

Analysis and Design Optimisation of Glass Structures

Modern architecture and construction industry utilises glass as an load bearing element. Building curtain wall facades and other prominent structures where glass is dominant material requires engineers and scientists to broaden the field of knowledge to cover modern material models, structural design methods and tools, etc.

Main goal of the study is to develop the methodology for an accurate analysis and design of glass panels and laminated glass composite panels.

The thesis is based on published articles.

The thesis is divided into four chapters. In chapter 1 first the features and application areas of the float, tempered and laminated glass structures are discussed. Next, an overview of optimization methods used in engineering design is given. Both, traditional gradient based and evolutionary nature based methods are discussed. Extra attention is paid to genetic algorithms, global optimization method, used most widely in engineering design. The multicriteria optimisation strategies and techniques are covered. The chapter 2 presents the experimental study regarding glass and laminated glass panels. The strength and stiffness characteristics are determined for glass and interlayers, also for laminated glass panel by applying the traditional mechanical (mostly for interlayer, where other approach are complicated) and modern nondestructive testing methods. Furthermore, an approach proposed for the measuring of normal residual stresses in glass proposed, allow to determine shear stresses (numerically) and estimate the error of normal stresses. The measurement of the normal residual stresses is performed in private company GlasStress according to proposed design of experiment. In chapter 3 the numerical methods for analysis of glass structures and its components are introduced. Main attention is paid on incorporation of the residual stresses in finite element simulation models. In chapter 4 the conclusion, covering the results obtained, is given.

The main goal of the study is achieved. The methodology for analysis of glass structures, based on combining theoretical analysis, experimental and numerical study, is proposed. Latter approach covers integration of the measured residual stresses in finite element simulation model. For the design optimization of glass canopy panel an advanced optimization procedure, based on combining artificial neural networks (ANN) and multicriteria genetic algorithms (GA), is developed.

The methodology proposed for analysis and design optimization of the glass structures has been tested/validated on particular glass structures with success and can be obviously extended for wider class of glass structures.

Lühikokkuvõte

Klaaskonstruksioonide analüüs ning optimeerimine

Kaasajal kasutatakse klaasi kandeelemendina nii arhitektuuris kui konstrueerimises laiemalt. Ehitiste fassaadide, keerukate ja prominentsete konstruksioonide projekteerimine, kus klaas on domineeriv materjal, eeldab inseneridelt ja teadlastelt teadmiste avardamist katmaks uusi materjalide mudelid, struktuuranalüüsi ja disaini meetodeid.

Käesoleva uurimistöö peamiseks eesmärgiks on metodoloogia väljatöötamine klaaspaneelide ja konstruksioonide täpsemaks/kaasaegseks analüüsiks ja optimeerimiseks.

Käesolev uurimistöö on artiklite põhine.

Uurimistöö on jaotatud neljaks peatükiks. Esimeses peatükis on kirjeldatud esmalt erinevate klaasi tüüpide (karastamata ja karastatud klaas, lamineeritud klaas) omadusi. Seejärel on antud ülevaade inseneerias enimkasutatavatest optimeerimise meetoditest, kattes nii traditsioonilised gradiendipõhised kui evolutsioonilised looduslikel protsessidel ja struktuuridel põhinevad meetodid. Eriline tähelepanu on pööratud geneetilistele algoritmidele, mis on inseneerias kõige laialdasemalt kasutatud globaalse optimeerimise meetod. Tutvustatud on ka multikriteeriaalse optimeerimise strateegiaid ja tehnikaid. Teises peatükis on kirjeldatud teostatud eksperimendilist uurimistööd. Jäikuse ja tugevuse omadused on määratud nii klaasi kihi kui ka laminaadi vahekihtide jaoks, rakendades traditsioonilisi mehaanikalisi (peamiselt õhukese sisekihi jaoks, kus muude tehnikate rakendamine on komplitseeritud) kui ka kaasaegseid mittepurustavaid tehnikaid. Töötati välja jääkpingete normaalkomponentide mõõtmise protseduur, mis võimaldab määrata (numbriliselt) ka nihkepinged ja anda veahinnangu normaalpingetele. Jääkpingete katseline mõõtmine teostati ettevõtte Glasstress poolt, võttes aluseks väljapakutud katseplaani. Kolmandas peatükis on kirjeldatud väljaarendatud simulatsioonimudeleid, pöörates peamise tähelepanu jääkpingete integreerimisele lõplike elementide simulatsioonimudelitesse. Neljas peatükk sisaldab tulemuste kokkuvõtet.

Töö peamine eesmärk on saavutatud. Töötati välja metodoloogia klaaspaneelide ja konstruksioonide analüüsiks, mis põhineb teoreetilise analüüsi, eksperimentaalsete uurimuste ja numbrilise analüüsi kombineerimisel. Viimane lähenemine võimaldab integreerida eksperimentaalsed määratud jääkpinged lõplike elementide simulatsiooni-mudelisse. Klaasist katusepaneeli optimeerimiseks töötati välja kaasaegne optimeerimise algoritm, mis põhineb tehisnärvivõrkude ja multikriteeriaalse geneetilise algoritmi kombineeritud kasutamisel.

Väljatöötatud metodoloogiat testiti edukalt konkreetsete klaaskonstruksioonide korral ja see meetodika on ilmselt laiendatav üldisema klassi klaaskonstruksioonide jaoks.

Appendix

Publication I

E. Õunapuu, T. Velsker, M. Eerme. (2015). Design optimization of glass canopy panel subjected to snow load. Proceedings of the 10th International DAAAM Baltic Conference "INDUSTRIAL ENGINEERING" (pp. 104–108). Tallinn: Tallinn University of Technology.

DESIGN OPTIMIZATION OF GLASS CANOPY PANEL SUBJECTED TO SNOW LOAD

Õunapuu, E.; Velsker, T.; Eerme, M.

Abstract:

The scope of this study is design optimization of glass canopy panel with prespecified strength properties and geometrical dimensions. The panel is subjected to snow load. Maximum Von Mises stresses and maximum deflection of the panel are considered as objective functions.

The stress-strain relationship of the glass canopy panel with point fixings is determined by use of FE analysis. A mathematical model for evaluation of objective functions is developed. Optimal set of design variables is determined based on preliminary analysis.

1. INTRODUCTION

Fast development in architecture has transformed glass from window material into load carrying element material. Glass canopy panels, floors and full glass facades are common in modern city buildings. Application of the point supported glass and FEM (finite element method) analysis have been the main reasons of expeditious development in the field.

The considered glass canopy panel represents thin glass layers with relatively large surface area. The glass layers have a certain amount of holes for point fixings. The main problems for designing such panels are large deflections of the panel and high stresses around fixing holes. The solution procedure proposed in the current study is based on combining the hybrid

genetic algorithms (HGA), meta-modelling techniques and FE analysis.

Among a large number of meta-modelling techniques available like regression methods [1, 2], kriging models [3, 4], splines & radial based functions [5, 6], etc., the feedforward artificial neural network techniques [7, 8] are selected due to their high accuracy and simplicity. The optimization procedure introduced can be regarded as extension of the optimization algorithms developed by workgroup for design of composite and sheet metal structures [9-12]. These multicriteria optimization algorithms are based on pioneering study in this area by Deb [13], Coello-Coello [14]. Deb et al. introduced nondominated sorting based NSGA2 algorithm with reduced computational complexity in [15]. Latter algorithm is widely used approach in design of optimization methods up to now. One new trend in design optimization of advanced engineering materials and structures is design of stiffness variables [16-20] (caused by advances in manufacturing technology).

The aim of the current study is to determine optimal configuration of glass canopy panel subjected to snow loading. Current study can be considered as extension of paper [21] containing preliminary design based on Taguchi design of experiment.

2. PROBLEM FORMULATION

The current study is focused on design optimization of glass canopy panel

subjected to snow loading (Figure 1).

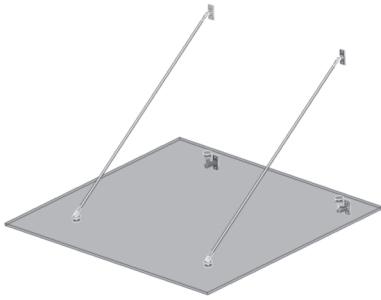
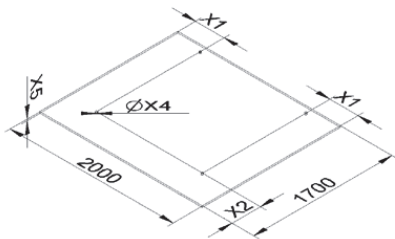


Fig. 1. Glass canopy with point supports

Design of such a structure is a complex task problem due to presence of mixed integer variables, rather specific stress-strain behaviour of glass and multiple constraints. The main characteristics considered in design of glass canopy panel are maximum stresses, maximum deflection and maximum strain energy density. These criteria are conditioned by the thickness of glass panel and the location and diameter of fixing holes.

The dimensions of the panel are given by the manufacturer of glass canopies which are 1700 mm in width and 2000 mm in length. The objective is search for an optimal set of design variables X1, X2, X4 and X5.



The design variable X3 is fixed in the current study based on results of preliminary design [21] and technological constraints. Panel is made of tempered soda lime silicate glass. It is assumed that the panel is made from monolithic solid glass, although common practice is to use two thinner glass panels laminated together. The variables X1 and X2 stand for the coordinates of the fixing holes, X4 is the diameter of the hole and X5 is the

thickness of the panel. Panel is subjected to gravity and pressure caused by snow load, no wind load is considered (Figures 2-3).

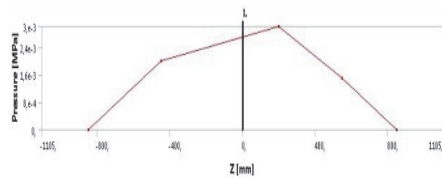


Fig. 2. Distribution of snow load

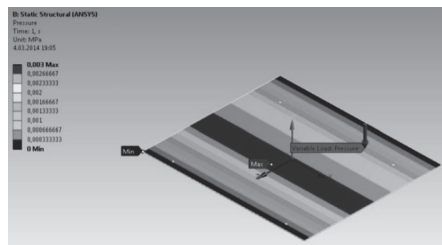


Fig.3. ANSYS Variable load pressure model

3. FINITE ELEMENT ANALYSIS

To analyse glass panel with point fixings, a three dimensional FEM model is applied. The deformation of the glass canopy panel subjected to snow load may exceed the thickness of the panel. Thereby the behaviour of the panel cannot be described accurately by linear theory. A nonlinear plate theory is applied. The stress-strain state of the glass panel is analysed with FEA software (ANSYS) where simulation model with solid elements has been developed. For avoiding long calculation times, the general mesh element size of the model is delimited with 20 mm. Due to fact the maximum stresses occur around the fixing holes, the size of mesh elements around the holes is decreased to 3 mm. Such mesh is employed around holes in 40 mm diameter sphere.

The values of the design variables are chosen based on manufacturing and structural limits. Four levels have been considered for the design variables X1, X2, X4 and three levels for X5, respectively.

The value of the variable X3 is fixed as mentioned above. Parametrical model according to the values of design variables was created in ANSYS Workbench.

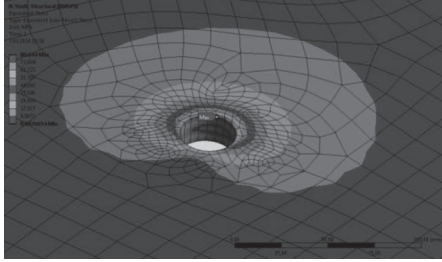


Fig. 2 Stresses around fixing holes

The maximum stresses occur on the edges of fixing holes.

4. DESIGN OPTIMIZATION

In the following, the output data obtained from FE analysis are treated as response values. However, the evaluation of the objective functions by means FE simulations is time consuming. A common technique for reducing computational cost in optimization algorithms is using surrogate models for approximation of the objective functions.

In the current study the artificial neural networks (ANN) based surrogate models are employed to guide the search towards a global optimum. The Marquardt-Levenberg algorithm has been applied for training of a two-layer backpropagation artificial neural network. This algorithm combines the advantages of the steepest descent (wider convergence domain) and Newton (higher convergence speed) methods. The configuration of the ANN has been tuned for particular problem. The radbas neurons and purelin neurons are used in first and second network layers, respectively.

The considered optimization problem is a mixed integer problem. The design variables X1 and X2, describing positions of the holes are real valued, but the radius of the hole and thickness have integer values. An analysis of the optimality

criteria has been performed and different formulations of the optimization problem are examined.

The minimization of the maximum value of the Von Mises stress and maximum deflection are considered as two criteria

$$f_1(\bar{x}) = \min(\sigma_{\max}^{VonMises}(\bar{x})), \quad (1)$$

subjected to

$$x_i \leq x_i^*, \quad -x_i \leq x_{i^*}, \quad i = 1, \dots, n, \quad (2)$$

$$\varepsilon_{\max}(\bar{x}) \leq \varepsilon_{\max}^*(\bar{x}), \quad (3)$$

$$C(\bar{x}) \leq C^*(\bar{x}) \quad (4)$$

and

$$f_2(\bar{x}) = \min(\varepsilon_{\max}(\bar{x})) \quad (5)$$

subjected to (2), (4) and

$$\sigma_{\max}^{VonMises}(\bar{x}) \leq \sigma_{\max}^{VonMises^*}(\bar{x}). \quad (6)$$

In (1)-(6) x_i stand for normalized design variables, \bar{x} is a vector of design variables, $\sigma_{\max}^{VonMises}(\bar{x})$ and $\varepsilon_{\max}(\bar{x})$ stand for normalized maximum values of Von Mises stress and deflection, respectively. The lower and upper limit values of the variables/functions are denoted by asterisk. These two objectives are nonconflicting and their application results a quite similar solutions shown in table (rows 2-3).

Table 2. Objective functions and optimal solutions

Objective	X1	X2	X4	X5
f_1	394.56	450.00	35	20
f_2	399.51	450.00	34	20
f_3	396.52	450.00	35	20

The objective $f_3(\bar{x})$ shown in last row of the Table 2 is defined as weighted sum of the objectives $f_1(\bar{x})$ and $f_2(\bar{x})$ as

$$f_3(\bar{x}) = w_1 f_1(\bar{x}) + w_2 f_2(\bar{x}). \quad (7)$$

Here the weights w_1 and w_2 determine the significance of the corresponding criteria

$$w_1 + w_2 = 1. \quad (8)$$

In Table 2 the values of the design variables are given in original dimensions in order to simplify understanding their real meaning.

The hybrid genetic algorithm (HGA) developed by workgroup for analysis of composite structures [7] is adapted for solving above considered mixed integer optimization problem. The genetic algorithm is applied for global search. Local search is performed by combining steepest descent and Branch and Bound methods.

5. DISCUSSION

The FEA results as well as optimization results are given in section 2 and 3, respectively. Three optimality criteria are examined. As it can be expected the first two criteria minimization of the maximum Von Mises stress and maximum deformations are not conflicting. Thus, the use of physical programming techniques for combining these criteria is justified (for conflicting criteria can be applied Pareto concept). Employing the weighted summation criterion (7) allows to consider two objectives but perform optimization with one combined objective. In comparison with objectives (1) and (5) here is less constraints necessary (on design variables only). The weights w_1 and w_2 can be assigned according to significance of the objectives (higher weight to more critical objective).

It can be seen from Table 2 that the values of the design variables corresponding to combined objective remains between the values of the single objectives (X1) or coincide with these values. Also, the optimal solutions corresponding to different criteria are close.

The values of the thickness (X5) are equal to upper limit since the cost is not considered as objective function and constraints on value of the cost (4) applied appears satisfied in the case of all optimal designs considered (in general increasing thickness improve mechanical performance but increase cost). The cost can be considered as objective in future study. The position parameter X5 also achieved upper limit value in the case of optimal designs determined. Here can be considered reconfiguring of the design domain for this variable.

6. CONCLUSION

A nonlinear FE analysis of the glass canopy panel subjected to snow load is performed. Based on FEA results the ANN based mathematical model is composed. The full factorial design of experiment technique has been applied for selection of input dataset. The HGA based multilevel optimization procedure is developed/ adapted for particular problem. Optimal configuration of the glass canopy panel subjected to given load case is determined. The results obtained by applying three different optimality criteria are close (see table 2). Introduction of additional optimality criterion – cost of the structure seems reasonable. The simulation models and optimization procedures developed can be applied for solving wider class of design problems.

7. REFERENCES

1. A. C. Rencher, W. F. Christensen. *Methods of Multivariate Analysis*. Third Edition. Wiley Series in Probability and Statistics. John Wiley & Sons, Inc. 2012.
2. T. P. Ryan. *Modern Regression Methods*. Wiley Interscience. 2011.
3. I. Pan, M. Babaei, A. Korre, S. Durucan, A multi-period injection strategy based optimisation approach using kriging meta-

- models for CO₂ storage technologies. *Energy Procedia*. 2014, 63 3492 – 3499.
4. K. Elsayed, C. Lacor, Robust parameter design optimization using Kriging, RBF and RBFNN with gradient-based and evolutionary optimization techniques. *Applied Mathematics and Computation* 2014, 236, 325–344.
 5. H.Cohen. *Numerical Approximation Methods*. Springer Science + Business Media LLC. 2011.
 6. J. Kers, J. Majak. Modelling a new composite from a recycled GFRP. In: *Mechanics of Composite Materials*, 2008, 44(6), p 623-632.
 7. H.Herranen, O.Pabut, M.Eerme, J.Majak, M.Pohlak, J.Kers, M.Saarna, G.Allikas, A.Aruiit. Design and Testing of Sandwich Structures with Different Core Materials. *Materials Science-Medziagotyra*, 2012, 18 , 1, 45-50.
 8. J.Majak, M.Pohlak, M.Eerme, T.Velsker. Design of car frontal protection system using neural networks and genetic algorithm. 2012, *Mechanika*, 4, 453-460.
 9. J.Majak, M. Pohlak. Optimal material orientation of linear and non-linear elastic 3D anisotropic materials. 2010. *Meccanica*, 45, 5, 671-680.
 10. J.Majak, M.Pohlak. Decomposition method for solving optimal material orientation problems. *Composite structures*. 2010, 92, 8, 1839-1845.
 11. J.Majak, S.Hannus, Orientational design of anisotropic materials using the Hill and Tsai-Wu strength criteria. *Mechanics of Composite Materials*, 2003, 39, 6, 509-520.
 12. J.Lellep, J. Majak, Nonlinear constitutive behaviour of orthotropic materials. *Mechanics of Composite Materials*. 2000. 36, 4, 261-266.
 13. K.Deb. *Multi-Objective Optimization Using Evolutionary Algorithms*. Wiley, M. 2009.
 14. CA. Coello Coello, GT.Pulido, A Micro-Genetic Algorithm for Multiobjective Optimization. *Evolutionary Multi-Criterion Optimization. Lecture Notes in Computer Science*, 2001, 1993, 126-140.
 15. K. Deb, A.Pratap , S.Agarwal, T. Meyarivan, A Fast Elitist Multi-Objective Genetic Algorithm: NSGA-II. *IEEE Transactions on Evolutionary Computation*. 2002, 6(2), 182-197.
 16. Y.Guo, M.Ruess, Z.Gürdal, A contact extended isogeometric layerwise approach for the buckling analysis of delaminated composites. *Composite Structures*. 2014, 16, 55-66.
 17. J.Sliseris, K.Rocens, Optimal design of composite plates with discrete variable stiffness. *Composite Structures*, 2013, 98, 15-23.
 18. J.Sliseris, G.Frolovs, K. Rocens, V.Goremikins, Optimal Design of GFRP-Plywood Variable Stiffness Plate. *Procedia Engineering*, 2013, 57, 1060-1069.
 19. J.Sliseris, H.Andrä, M.Kabel, B.Dix, B.Plinke, O.Wirjadi, G. Frolovs, Numerical prediction of the stiffness and strength of medium density fiberboards. *Mechanics of Materials*, 2014, 79, 73-84.
 20. A. Khani, M.M. Abdalla, Z. Gürdal, Optimum tailoring of fibre-steered longitudinally stiffened cylinders, *Composite Structures*, 2015, 122, 343-351.
 21. T.Velsker, H.Lend, M.Kirs. Design of glass canopy panel. *Proceedings of the 8th International Conference DAAAM Baltic Industrial engineering*, 2012, 759 – 764.

Publication II

K. Väer, J. Anton, A. Klauson, M. Eerme, E. Öunapuu, P. Tšukrejev. (2017). Material Characterization for Laminated Glass Composite Panel. *Journal of Achievements in Materials and Manufacturing Engineering*, 81, 11–17.

Material characterization for laminated glass composite panel

K. Väer ^{a,*}, J. Anton ^b, A. Klauson ^c, M. Eerme ^a, E. Õunapuu ^a, P. Tšukrejev ^d

^a Department of Mechanical and Industrial Engineering, Tallinn University of Technology, Ehitajate tee 5, 19086 Tallinn, Estonia

^b GlasStress Ltd, Akadeemia tee 21, 12618 Tallinn, Estonia

^c Department of Civil Engineering and Architecture, Tallinn University of Technology, Ehitajate tee 5, 19086 Tallinn, Estonia

^d Estonian Entrepreneurship University of Applied Sciences Mainor, Suur-Sõjamäe 10a, 11415 Tallinn, Estonia

* Corresponding e-mail address: kaur.vaer@ttu.ee

ABSTRACT

Purpose: Laminated glass composite panel (LGCP) with at least one flexible plastic/viscoelastic interlayer is considered. The purpose of this paper is to determine the material properties of the constituents of LGCP required for accurate modelling of the laminated glass structures.

Design/methodology/approach: The proposed approach includes the following three type of tests: non-destructive tests for determining mechanical properties of the glass layers (based on wave propagation), mechanical tests and finite element simulations for determining properties of the interlayers, measuring residual stresses in glass layers using novel methods and equipment (non-destructive, wave propagation based).

Findings: Methodology and procedures for determining material properties of the LGCP.

Research limitations/implications: Due to fact that the shear moduli of the viscoelastic interlayers and glass skin layers differs up to thousands times, the direct application of the classical sandwich theory may lead to inaccurate results. The layer wise plate theory with viscoelastic interlayer should be applied. In the case of layer wise theory, the material properties should be determined for each layer (not averaged properties for laminate only).

Practical implications: The proposed approach allows to determine the properties of the LGCP components with high accuracy and form base for development of accurate plate model for modelling vibration, buckling and bending of the LGCP. The effect of the residual stresses is most commonly omitted in engineering applications. However, in the case of tempered glass the residual stresses are significant and have obviously impact on stress-strain behaviour of the laminated glass panel.

Originality/value: Study consists of valuable parts, i.e. determining residual stresses in glass performed in cooperation with private company GlasStress Ltd. Special software and measuring equipment are developed. Further LGCP interlayer mechanical properties are tested experimentally and using simulation tools for design optimization purposes.

Keywords: Laminated glass composite panel; Non-destructive testing; Interlayer mechanical properties; Measuring residual stresses

Reference to this paper should be given in the following way:

K. Väer, J. Anton, A. Klauson, M. Eerme, E. Öunapuu, P. Tšukrejev, Material characterization for laminated glass composite panel, Journal of Achievements in Materials and Manufacturing Engineering 81/1 (2017) 11-17.

ANALYSIS AND MODELLING

1. Introduction

Laminated glass composite panel (LGCP) with at least one flexible interlayer is considered.

The strengthening interlayer provides better post failure safety of LGCP due to ability to hold broken-off pieces of glass together. Commonly used interlayers include polyethylene terephthalate, polyvinyl butyral, ethylene-vinyl acetate, also transparent thermoplastic materials. The acoustic interlayer in form of acoustic film, micro-perforated materials, etc., provides sound attenuation capabilities. Multifunctional LGCP with improved strength and acoustic performance can be obtained by combining strengthening and acoustic interlayer or using novel acoustic interlayers covering strengthening and sound attenuation properties.

The multifunctional laminated glass composite panels are used as windows of the vehicles, transparent walls in buildings, etc.

It should be pointed out that the properties of the interlayers are different before and after manufacturing of the LGCP due to high temperature treatment effects. Thus, there is need to perform the manufacturing process in such a manner that the interlayer can be separated after manufacturing in order to evaluate/measure its properties. Detailed description of the evaluation of the interlayers are given in section 2.3.

The thermal treatment of the glass sheets will improve strength properties, but cause also residual stresses, which are discussed in details in section 2.2.

In the case of three layer LGCP the classical sandwich theory with certain adaptation/ modification can be applied. Main features of the LGCP structures can be outlined as:

- top and bottom layers consist from one glass layer,
- interlayer is a multilayer laminate or one multifunctional layer,
- top and bottom glass layer are thick and interlayer is thin (contra dictionary to traditional sandwich structures),
- interlayer has complex material properties (plastic, viscoelastic),
- here are significant residual stresses in tempered glass layers,

- the ratio of shear moduli of the core and skin is extremely small (between 10⁻⁵ and 10⁻²).

Due to above listed features of the LGCP structures the direct application of the classical sandwich theory may lead to inaccurate results.

In [1-3] the classical sandwich theory is adapted for analysis of LGCP. The system of PDE providing extension to the classical plate theories has been derived in [1] based on layer-wise theory approach. Applicability of the first order shear deformation theory is analysed in [2] based on results of higher order layer-wise theory. In [3] the finite element formulation based on layer-wise theory and user-defined element has been introduced.

Viscoelastic interlayer, usually polyvinyl butyral (PVB) improves adhesive strength of laminated glass composite panel (LGCP). The advantages reveal under impact shock, where the interlayer bears large displacements and holds the shattered glass pieces together for safety glass applications.

Some experimental and numerical studies have been carried out to determine the tensile properties of PVB interlayer and PVB interlayer in LGCP. Fors [4] concluded interlayer thickness to have minor influence on tensile properties at time-dependant stress-strain experiments. Zhang [5] introduced hyperelastic material deformation under quasi-static tensile loading at high-strain conditions for PVB. Molnar [6] observed in his finite-element parametric study that after structural configurations a thinner soft PVB interlayer film improves glass panel rigidity significantly. Zang modelled impact damage in laminated glass panel using finite element method by means of PVB thickness and material parameters on stress wave propagation [7].

This study concentrates on determining material properties of LGCP panel layers as the properties of the LGCP panel are determined by its constituents. The non-destructive testing methods are preferred as resource saving and sustainable. The PVB interlayers have key role in aging of LGCP laminates and need special attention since in a number of application long term exploitation of LGCP panels has been foreseen (solar panels, windows). The elastic material properties of the PVB interlayer determined

experimentally are used as simulation input parameters in order to predict vibration attenuation capability at concurrent frequency excitation and displacement.

2. Experimental study

As mentioned above, for proper modelling of the laminated glass panel first is needed to determine properties of its constituents. In the following sections the three type of tests have been performed. The non-destructive test methods are applied for determination mechanical properties of the glass layer, also residual stresses in glass. The mechanical properties of the interlayer are determined by tensile tests.

2.1. Determination of material properties of the glass layer by acoustic method

In the test sound speeds of P-wave and shear wave are determined by the measurement of the time of flight of the individual pulses. The signal is generated by JSR DPR300 pulse generator (Fig. 1). Piezoelectric broadband contact transducer Olympus M110 (central frequency 5 MHz) is used to generate P-wave and transducer V151 (central frequency 0.5 MHz) to generate shear wave. Reflected pulses are visualized on the oscilloscope and time lag between two consecutive pulses is measured.

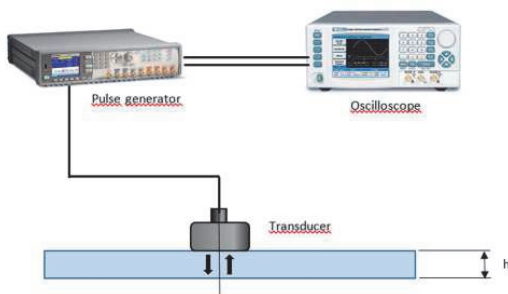


Fig. 1. Set up for measuring P-wave and shear wave speeds

Table 1.

Measured wave speeds and computed elastic properties of the glass layers (float and tempered glass)

	h , mm	ρ , kg/m ³	c_p , m/s	c_s , m/s	G , GPa	E , GPa	ν , -
Float glass	7.88	2486±3	5914±39	3506±5	30.55±0.5	75.11±0.5	0.23±0.01
Tempered glass	7.92	2486±7	5852±58	3433±2	29.30±0.1	72.53±0.5	0.24±0.01

Thus, obtained speeds of P-wave and shear waves make it possible to determine Young modulus E and Poisson ratio ν as

$$E = \frac{G(3M - 4G)}{M - G}, \quad (1)$$

$$\nu = \frac{M - 2G}{2M - 2G}, \quad (2)$$

where M and G stand for the bulk and shear modulus, respectively

$$M = c_p^2 \rho, \quad G = c_s^2 \rho. \quad (3)$$

In (3) c_p and c_s stand for the wave speeds and ρ is a material density.

The elastic properties of the glass layer computed by formulas (1)-(3) are shown in Table 1.

It can be observed from Table 1 that the values of the Young and shear modulus are higher in the case of the float glass, but the difference is relatively small (less than 5%). The value of the Poisson ratio is higher in the case of tempered glass (difference also less than 5%).

2.2. Determination of residual stresses in glass layer

Annealed and heat treated single and laminated soda lime glass plates are tested. The design of experiment has been performed in Tallinn University of Technology and tests in private company GlasStress Ltd. GlasStress SCALP-05 and scattered light method was used to determine through-the-thickness stress distribution. Sample pictures were taken between crossed polarisers. Tin side of the glass was detected with Tin Side Detector UV1301. The residual stresses were measured on both sides of the glass. Perpendicular measurements were done in the centre of glass. For better reliability 3 repeatable measurements were done in each direction. Average surface stress was measured at 10 different locations on glass surface.

First were measured the through-the-thickness residual stresses in float glass from air side (Fig. 2) and tin side (Fig. 3). Here air side is a free upper side of the glass during manufacturing process and tin side is opposite side (in contact).

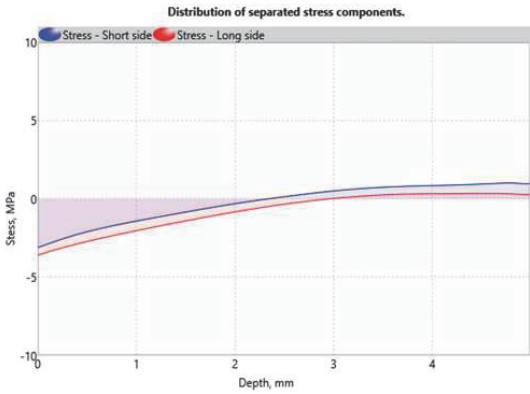


Fig. 2. Through-the-thickness residual stresses distribution in float glass (measured from air side)

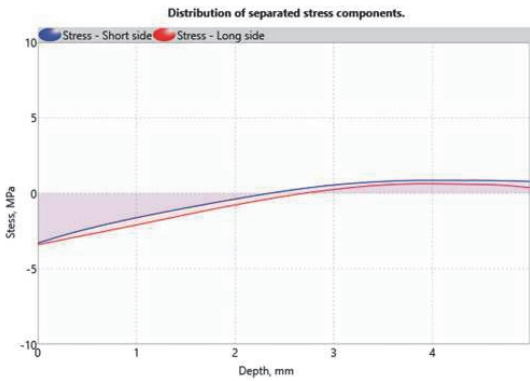


Fig. 3. Through-the-thickness residual stresses distribution in float glass (measured from tin side)

The stresses are measured from both sides (air and tin) up to middle surface with small reserves. The red and blue lines stand for stress components σ_1 and σ_2 , respectively. Note that these components are just stresses along long and short side of the laminated glass specimen and not necessarily principal stresses. The stresses are negative (compression) near surfaces and positive (tension) near middle surface. Also, in the case of float glass the residual stresses remain small (less than 5 MPa). In Figures 4 (air side) and 5 (tin side) the through-the-thickness residual stress distribution is given for tempered glass.

Obviously, the values of the residual stresses are significantly higher. The surface stresses achieve the values $\sigma_1 = -89.4$ MPa, on $\sigma_2 = -89.9$ MPa on tin side and

$\sigma_1 = -88$ MPa, on $\sigma_2 = -89.1$ MPa on air side. Similarly, to float glass the compression and tension stresses are observed near surface and middle surface, respectively.

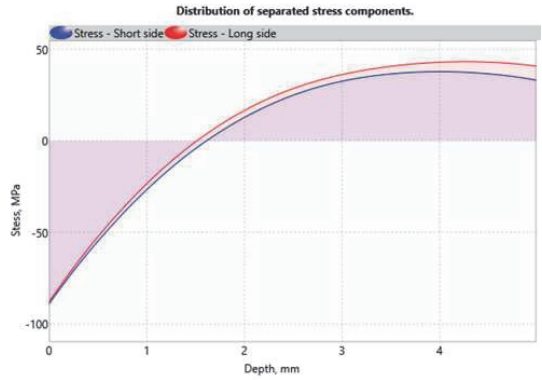


Fig. 4. Through-the-thickness residual stress distribution in tempered glass (measured from air side)

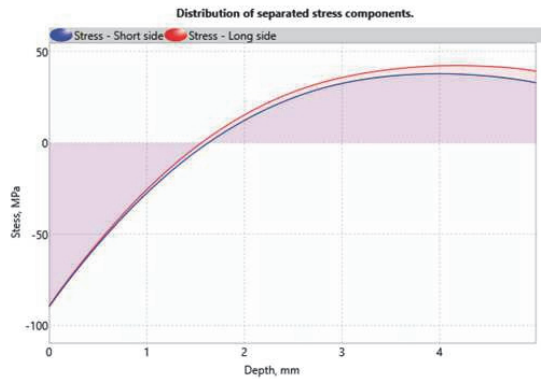


Fig. 5. Through-the-thickness residual stress distribution in tempered glass (measured from tin side)

2.3. Determination of the material properties of polyvinyl butyral (PVB) interlayer

The acoustic evaluation of the material properties of PVB as done above for glass layer is complicated due to small thickness and damping properties of the PVB layer. For that reason, the elastic properties of the interlayer are determined from tensile tests. Several standardized mechanical tests were carried out to characterize stiffness and tensile properties of PVB interlayer. An Instron Series

5800 electromechanical test system was used with original mechanical clamping grips, where friction-induced slips between interlayer-grip were restrained. Specimen type 5 (Fig. 6) from ISO-527-3 [9] was chosen carefully due to the fracture occurring towards specimen centre with minor fixture influence at repetitive experiments. Any broken sample parts inside fixtures were not present. PVB sheets of 0.76 mm were used to determine stiffness and tensile properties depending on interlayer material type and treatment.

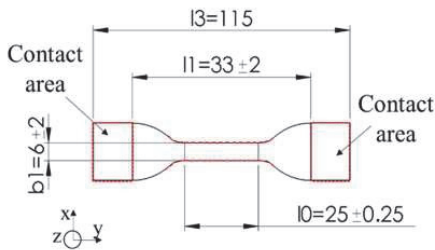


Fig. 6. Specimen geometry characteristics for determining stiffness and tensile properties (mesh refinement areas for consecutive FE-simulation are marked with red)

The tests were carried out at three different speeds 500, 200 and 10 mm/min with reference to ISO-527-1 [8] and ISO-527-3 [9] at room temperature. Young's modulus was defined at initial slope of the stress-strain curve in between strain $\varepsilon_1 = 0.0005$ and $\varepsilon_2 = 0.0025$ using regression methodology in PC integrated to measuring equipment. Maximum values for tensile stress and strain were determined at curve end, material breaking point.

Table 2.

Mechanical test results of Young's modulus, tensile stress and tensile strain at break at three different speeds for 0.76 mm PVB

Speed rate, mm/min	Young's modulus, MPa			
	PVB	Acoustic PVB	Heat treated PVB	Heat treated acoustic PVB
500	2.42±0.11	2.67±0.05	2.16±0.11	2.52±0.07
200	1.56±0.07	1.97±0.05	[-]	[-]
10	0.97±0.08	0.99±0.02	0.75±0.03	0.85±0.04
Tensile stress at break, MPa				
500	23.89±0.03	20.33±0.05	22.15±0.10	17.96±0.12
200	24.03±0.06	20.56±0.06	[-]	[-]
10	21.34±0.09	15.63±0.08	19.70±0.04	14.77±0.01
Tensile strain at break, %				
500	488.05±0.05	425.86±0.04	444.36±0.07	394.74±0.07
200	518.55±0.05	453.90±0.05	-	-
10	588.76±0.04	555.68±0.05	607.32±0.02	519.52±0.01

Experimental results shown in Table 2 are obtained based on 3-5 repetitive runs. All stress-strain curves show more or less a polynomial shape (example is given in Fig. 7). Stiffest material properties were determined for acoustic PVB, where the difference between untreated PVB is stronger at low strain conditions, 500 and 200 mm/min. Conversely, heat treatment reduced stiffness of PVB sheets 10.8% and 5.7% for PVB and acoustic PVB, respectively.

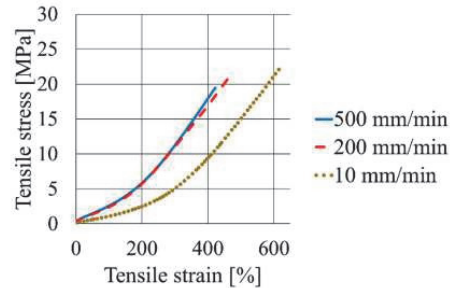


Fig. 7. Tensile stress-strain graph (untreated PVB 0.76 mm)

The pressure required to break the PVB sheets was determined as tensile stress at breaking point. Results were strongly time-dependant, similarly to Young's modulus. Strongest time-influence for maximum tensile stress from 500 until 10 mm/min testing speed was observed for acoustic PVB. Constant stress at almost constant strain is observed for 10 mm/min testing speed for all PVB material types, referring to creep. There, heat treated samples possessed slightly deeper curve slope during initial elongation, referring to larger displacement, than other material types.

Heat treatment of PVB improved tensile strain properties at high strain (testing speed 10 mm/min) conditions by 27%. However, it was also observed that heat treatment had minor and unfavourable effect on stiffness for acoustic heat treated and only heat-treated PVB sheets respectively.

High-scale tensile strain and small-scale tensile stress values at testing speed 10 mm/min are due to more time used for energy conversion. In energy conversion, it is meant that accumulated kinetic energy during motion was converted to potential energy, that was finally released at point of fracture. Highest tensile strain was observed at 10 mm/min testing speed because lower strain density revealed less stresses during elongation. It is concluded, when improving both stiffness and tensile properties, acoustic interlayer properties had higher influence than heat treated interlayer properties.

3. Finite element simulation of PVB interlayer

Time-dependent strain, obtaining physical sample shape after fracture and tendency to creep at these transient experiments refer to PVB viscoelastic material property. Viscoelasticity means possessing viscous and elastic properties when undergoing deformation, that result in extended tensile elongation, major sound and vibration attenuation for laminated glass composite panel (LGCP). To gain new data supporting viscoelasticity, incl. vibration attenuation, finite element simulations were carried out at concurrent steady state oscillation and strain excitation. Dynamic finite element simulation conditions were prepared including obtained Young's modulus experimental values at low strain conditions as input parameters (all material properties are given in Table 3).

Table 3.

Material properties for PVB (simulation input for modal and harmonic analysis)

Mass density, g/cm ³	Young's modulus, MPa	Poisson ratio, -
1.07	2.42	0.45

Mesh discretization with denser element density (denser mesh with 3/1 ratio respect to other area) on contact area faces and geometry transition edges (see positioning in Fig. 6) resulted with a total of 36 243 elements. Amount of 4 elements through sample thickness on said areas restrained mathematic singularities that may occur due to

finite element idealizations. Modal analysis was carried out at completely fixed conditions for contact areas to reveal dynamic response of specimen. These results consisted of mode shapes and frequencies. The irregularity in mode shapes is caused by nonlinear sample shape and boundary conditions. This resulted in imbalanced mass fractions on different geometry locations. The results also determined the excitation frequency range for harmonic analysis, that is carried out with ten solution intervals through frequency spectrum. For simplification, here same experimental boundary conditions were built up in harmonic simulation model. Rotations at each direction respect to global coordinate system were restrained as default at four fixing facets. Translative movement of sample was restrained at one end ($U_x=U_y=U_z=0$) to prevent rigid body motion. At other end, tensile extension as displacement at low strain 500 mm/min ($U_y=139.4$ mm, $U_x=U_z=0$) was applied corresponded to forcing frequency. Full harmonic analysis conditions were implemented for manufactured PVB thicknesses due to displacement condition. In results (given in Fig. 8) it is observed a gradual amplitude decrease as function of layer thickness.

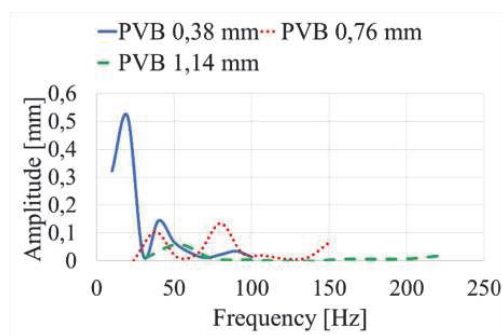


Fig. 8. FE-simulation results: displacement amplitude plotted against forcing frequency

The added mass caused almost oscillation attenuation when reaching PVB thickness 1.14 mm at same stiffness conditions. Largest amplitude values are located between $20 \text{ Hz} \leq a_{\max} \leq 80 \text{ Hz}$ regardless of layer thickness.

The future study is related with design optimization of multifunctional glass laminated composite panels (thicknesses and materials of layers, stacking sequence, heat treating). The multi-criteria global optimization methods based procedures and algorithms developed by workgroup for design various composite materials and structures [10-15] can be adopted for particular problem considered.

4. Conclusions

The material properties of LGCP layers are determined experimentally. Advanced equipment and software are employed for measuring residual stresses in glass layer. GlasStress SCALP-05 and scattered light method was used to determine through-the-thickness stress distribution. This detailed and valuable information can be used in future analysis and design of LGCP panels. The residual stresses are often omitted in structural analysis or used some estimated values. However, in the case of tempered glass the residual stress values measured in range of 90 MPa and have obviously impact of structural analysis results.

The elastic material properties of the glass layer are determined by acoustic method avoiding producing waste and providing sparingly use of materials.

The destructive tensile tests are used for determining material properties of the PVB interlayer, since here is complication to apply non-destructive methods due to thin layers and higher damping properties. However, certain non-destructive tests of the PVB layer are in progress. Steady state harmonic analysis revealed major vibration attenuation capability for PVB layer with 1.14 mm thickness at combined vibration excitation and displacement conditions.

The experimental results obtained form basis for accurate analysis and design of LGCP panels.

Acknowledgements

The research was supported by Estonian Research Council grant PUT1300; Estonian Centre of Excellence in Zero Energy and Resource Efficient Smart Buildings and Districts, ZEBE, TK146 funded by the European Regional Development Fund (grant 2014-2020.4.01.15-0016); Innovative Manufacturing Engineering Systems Competence Centre IMECC (supported by Enterprise Estonia and co-financed by the European Union Regional Development Fund, project EU48685).

References

- [1] K. Naumenko, V.A. Eremeyev, A layer-wise theory for laminated glass and photovoltaic panels, *Composite Structures* 112 (2014) 283-291.
- [2] J. Eisenträger, K. Naumenko, H. Altenbach, H. Köppe, Application of the first-order shear deformation theory to the analysis of laminated glasses and photovoltaic panels, *International Journal of Mechanical Sciences* 96-97 (2015) 163-171.
- [3] J. Eisenträger, K. Naumenko, H. Altenbach, J. Meenen, A user-defined finite element for laminated glass panels and photovoltaic modules based on a layer-wise theory, *Composite Structures* 133 (2015) 265-277.
- [4] C. Fors, *Mechanical Properties of interlayers in laminated glass*, Master thesis, Lund University, 2014.
- [5] X. Zhang, H. Hao, The mechanical properties of Polyvinyl Butyral (PVB) at high strain rates, *Construction and Building Materials* 93 (2015) 404-415.
- [6] G. Molnar, L. Vigh, L. Dunai, Finite element analysis of laminated structural glass plates with polyvinyl butyral (PVB) interlayer, *Periodica Polytechnica Civil Engineering* 56/1 (2012) 35-42.
- [7] S. Chen, M. Zang, D. Wang, Z. Zheng, C. Zhao, Finite element modelling of impact damage in polyvinyl butyral laminated glass, *Composite Structures* 138 (2016) 1-11.
- [8] Technical Committee ISO/TC 61, ISO 527-3: Determination of tensile properties (test conditions for films and sheets), International Organization for Standardization, Geneva, Switzerland, 1995.
- [9] Technical Committee ISO/TC 61, ISO 527-1: Determination of tensile properties (general principles), International Organization for Standardization, Geneva, Switzerland, 1993.
- [10] J. Lellep, J. Majak, On optimal orientation of nonlinear elastic orthotropic materials, *Structural Optimization* 14 (1997) 116-120.
- [11] J. Majak, S. Hannus, Orientational design of anisotropic materials using the Hill and Tsai-Wu strength criteria, *Mechanics of Composite Materials* 39/6 (2003) 509-520.
- [12] A. Aruniit, J. Kers, J. Majak, A. Krumme, K. Tall, Influence of hollow glass microspheres on the mechanical and physical properties and cost of particle reinforced polymer composites, *Proceedings of the Estonian Academy of Sciences* 61/3 (2012) 160-165.
- [13] H. Herranen, G. Allikas, M. Kirs, K. Mädamürk, Visualization of strain distribution around the edges of a rectangular foreign object inside the woven carbon fibre specimen, *Estonian Journal of Engineering* 18/3 (2012) 279-287.
- [14] M. Pohlak, J. Majak, M. Eerme, Optimization of Car Frontal Protection Systems, *Proceedings of the 6th International Conference of DAAAM Baltic Industrial Engineering*, 2008, 123-128.
- [15] K. Karjust, M. Pohlak, J. Majak, Technology route planning of large composite parts, *International Journal of Material Forming* 3 (2010) 631-634.

Publication III

E. Öunapuu, J. Anton, A. Klauson. Modelling residual stresses in glass structures. AIP Conference Proceedings 2116, 330007 (2019).

Modelling Residual Stresses in Glass Structures

Erko Õunapuu^{1, a)}, Johan Anton^{2, b)}, Aleksander Klauson^{3, c)}

¹ Department of Mechanical and Industrial Engineering, Tallinn University of Technology, Estonia

² Department of Civil Engineering and Architecture, Tallinn University of Technology, Estonia

³ Department of Cybernetics, Laboratory of Solid Mechanics, Tallinn University of Technology, Estonia

^{a)} Corresponding author: erko@rfix.eu

^{b)} Johan@ioc.ee

^{c)} Aleksander.Klauson@ttu.ee

Abstract. Nowadays the heat treated glass is widely used in civil engineering, automobile, space and marine applications due to its high strength properties in comparison with float glass. However, tempering leads to formation of residual stresses in glass which are often/commonly omitted in structural analysis of the glass. The aim of the current study is to determine experimentally residual stresses in tempered glass and to develop an advanced finite element simulation model for structural analysis of tempered glass utilizing measured residual stresses.

INTRODUCTION

The float glass splits into large fragments at breakage, but tempered glass usually breaks into small pieces [1]. The tempering/cooling process has a significant impact on mechanical performance of the material including its strength [2]. The residual stresses arise in glass during cooling down from the crystallization temperature. The residual stresses are caused by the thermal expansion and the elastic mismatch between the crystalline and glassy phases [3]. The ultimate bending strength of thermally untreated glass is estimated to be 20 MPa. Heat treating the glass rises the bending stress up to 6 times. Heat strengthening expands glass bending strength to maximum 70 MPa and tempering to maximum 120 MPa [4]. The strengthening effect is achieved with accurate cooling the glass after heat treatment. The fast cooling causes outer layers of the glass to compress and close micro cracks in the surface of the glass. To break the glass under tensile force these compressive stresses should be exceeded. The core of the glass remains under tension (FIGURE1).

The heat treated glass is used in applications with elevated snow and wind load and in applications with safety glass requirements [4]. The heat treated glass is also used in structures where glass is the main load bearing element such as glass fin facades, glass roofs etc. most commonly as layers of laminated glass composite panel (LGCP). The LGCP consists of glass layers and at least one flexible interlayer. The interlayer provides higher post failure safety of LGCP due to ability to hold broken-off pieces of glass together. Widely used interlayers can be outlined as polyethylene terephthalate, polyvinyl butyral, ethylene-vinyl acetate [4,5]. One particular emerging application of the LGCP is solar panel manufacturing [6-7]. In sound attenuation applications are employed acoustic interlayer in form of acoustic film, micro-perforated materials, etc. Multifunctional LGCP with improved strength and acoustic performance can be obtained by using novel acoustic interlayers covering strengthening and sound attenuation properties simultaneously. In the case of glass structures the sound attenuation is challenging problem. Emerging research area is development of new sound absorptive element for wide class of structures and applications [8-11].

In the current study the know-how and capabilities of the private company GlasStress Ltd in area of experimental study of residual stresses in glass structures [12-14] are combined with workgroup experiences in area of structural analysis and design optimization [15-19].

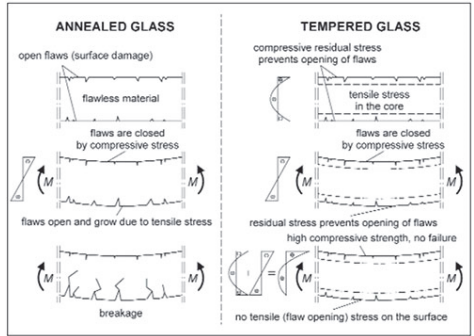


FIGURE1. Tensile forces applied to annealed(float) and tempered glass

The following sections cover experimental detection and numerical modelling of residual stresses.

EXPERIMENTAL STUDY

The experimental study was performed in cooperation with private company GlasStress Ltd using scattered light polariscope SCALP-05 developed by GlasStress Ltd. Samples 500x200 mm with different thicknesses are measured from both sides up to middle surface with small reserves. The setup of experimental analysis is shown on FIGURE 2. Three different sample thicknesses of tempered glass are tested: 4mm, 8 mm and 4+4 mm laminated glass with 0,38 mm PVB interlayer.



FIGURE 2. Measuring residual stresses with scattered light polariscope SCALP-05

The normal stress components σ_1 and σ_2 , aligned along long and short side of the glass specimen were measured through-the-thickness with 0,01 mm step size. In Figure 3 the values of the σ_1 through thickness of the glass specimen are depicted. The measurements performed from air and tin sides were combined into one curve.

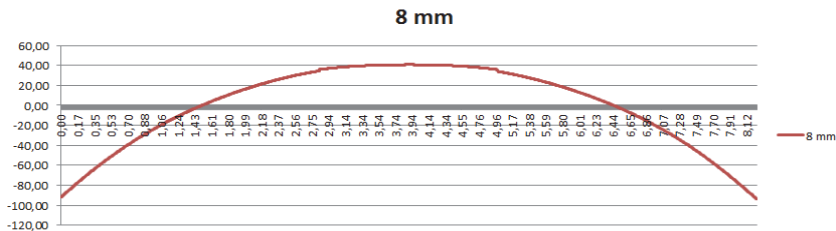


FIGURE 3. Through-thickness distribution of the stress component σ_1

In order to provide input data for stress tensor in numerical modelling the stress components σ_1 and σ_2 were measured additionally in coordinate system rotated 45° with respect to initial system (initial system is determined by long and short sides of the glass specimen). The shear stress σ_{12} was determined by applying stress tensor rotation formulas. Out of plane residual stresses are neglected.

FINITE ELEMENT SIMULATION MODEL

The experimental data obtained were utilized in finite element analysis (FEA) as input data. The FEA was performed using ANSYS v14. The solid elements were employed for controlling mesh size in all directions. Due to symmetry consideration only 1/8 of the sample was modelled. The linear motion of cut surfaces was constrained along surface normal. The model was divided into five plies through thickness. Layers of mesh nodes were selected separately, on each layer was applied initial state stress according to the experimental results (FIGURE 4). The user-defined snippet was developed for importing the stress data.

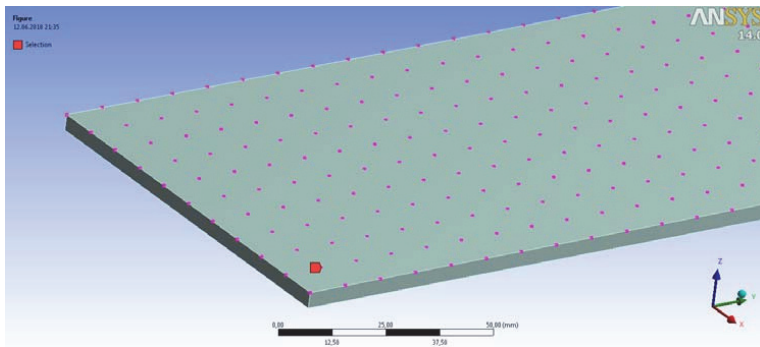
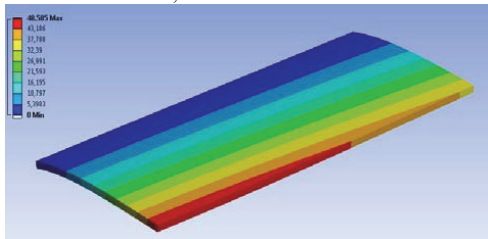


FIGURE 4. Applying initial state of stress on selected one layer of mesh nodes

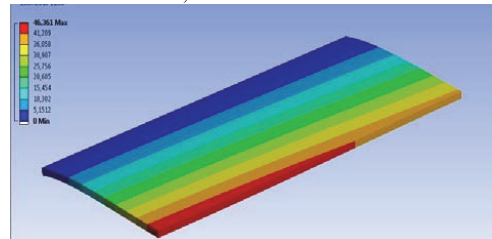
The FEA model including prestresses was treated for determining the change in natural frequencies in comparison with reference model with non-prestressed glass. The longer edge of the glass specimen was fixed and other edges were free.

Non-prestressed
Mode 1 - 221.58 Hz; 48.6 mm deformation



(a)

Prestressed
Mode 1 - 304.58 Hz; 46.4 mm deformation



(b)

FIGURE 5. Natural frequencies and displacements of the non-prestressed a) and prestressed b) glass

The rise of the natural frequencies of the prestressed specimen has been observed (FIGURE 5). The values of the deformations decreased, but the change was less substantial than that of natural frequencies. The validation of the numerical analysis is in progress. Future study is related with strength evaluation and design optimization of laminated glass composite panel [20-24].

CONCLUSIONS

The finite element simulation model covering the effect of residual stresses was developed for structural analysis of the glass panels. The residual stresses incorporated in FEA model were determined experimentally in cooperation with private company GlasStress Ltd using scattered light polariscope SCALP-05. It has been shown that in the case of tempered glass the residual stresses have significant influence on values of the natural frequencies. The proposed procedure for implementation of the residual stress can be applied for wide class of structural analysis and optimal design problems of glass structures. However, certain adaptation of the user-defined snippet related with geometry and material of the structure, boundary conditions, etc. may be needed. Besides, experimental study and FEM analysis performed the development of semi analytical structural design models has been foreseen in future study. The algorithms and tools provided for plate/shell structures can be adopted for laminated glass panels

ACKNOWLEDGMENTS

The authors acknowledge Innovative Manufacturing Engineering Systems Competence Centre IMECC (supported by Enterprise Estonia and co-financed by the European Union Regional Development Fund, project EU48685); the Estonian Centre of Excellence in Zero Energy and Resource Efficient Smart Buildings and Districts, ZEBE, TK146 funded by the European Regional Development Fund (grant 2014-2020.4.01.15-0016); Estonian Research Council grant PUT1300.

REFERENCES

- [1] M. Haldimann, A. Lubile A and M. Overend, Structural Engineering Documents, **10**. IABSE, Zürich, (2008).
- [2] M. Kotoul, J. Pokluda, P. Sandera, I. Dlouhí, Z. Chlup, A.R. Boccaccini, *Acta Mater.*, **56**, 2908–2918 (2008).
- [3] F.C. Serbena, E.D. Zanotto, *Journal of Non-Crystalline Solids*, **358**, 6–7, 975-984 (2012).
- [4] M. Fröling, Strength Design Methods for Glass Structures, Doctoral Thesis, (2013).
- [5] X. Zhang H. Hao, *Construction and Building Materials*, **93**, 404-415, (2015).
- [6] K. Naumenko, V. A. Eremeyev, *Composite Structures*, **112**, 283–291, (2014).
- [7] J. Eisenträger n, K. Naumenko, H. Altenbach, H. Köppe, *Int. J. of Mech. Sci.*, **96-97**, 163–171, (2015).
- [8] F. Auriemma, H. Rammal, J. Lavrentiev, *SAE Int. J. of Materials and Manufacturing*, **1** (1), 600–611 (2014).
- [9] F. Auriemma, *Applied Acoustics*, **122**, 128-137 (2017).
- [10] F. Auriemma, *Acoustics Australia*, **45** (2), 411-419 (2017).
- [11] F. Auriemma, Proc. of Meetings on Acoustics Meeting of Acoustical Society of America, **30**, 1, (2017), (Acoustics 2017 and 8th Forum Acusticum; Boston; United States; 25 June 2017 through 29 June 2017).
- [12] S. Hödemann, A. Valdmann, J. Anton, T. Murata, *J. of Materials Sci.*, **51** (12), (2016), 5962–5978.10.1007/s10853-016-9897-4.
- [13] H. Aben, J. Anton, M. Öis, K. Viswanathan, C. Chandrasekar, M. M. Chaudhri, *Applied Physics Letters*, **109**, 231903-1–231903-4.10.1063/1.4971339 (2016).
- [14] H. Aben, D. Locheignies, Y. Chen, J. Anton, M. Paemurru, M. Öis, *Experim. Mech.*, **55** (2), (2015) 483–486.
- [15] J. Lellep, J. Majak, *Structural Optimization*, **14**, 116-120 (1997).
- [16] J. Lellep, J. Majak, *Mechanics of Composite Materials*, **36** (4), 261–266 (2000).
- [17] A. Aruniit, J. Kers, J. Majak, A. Krumme, K. Tall, *Proc. of Estonian Acad. of Sci.*, **61**(3), 160-165 (2012).
- [18] K. Karjust, M. Pohlak, J. Majak, *Int. J. of Material Forming*, **3**, 631–634 (2010).
- [19] A. Aruniit, J. Kers, D. Goljandin, M. Saarna, K. Tall, J. Majak, H. Herranen, *Materials Science (Medžiagotyra)*, **17** (3), 276-281 (2011).
- [20] J. Šliseris, K. Rocens, *World Acad. of Sci., Eng. and Tech.*, **76**, 317-323 (2011).
- [21] J. Šliseris, K. Rocens, *J. of Civil Eng. and Management*, **19** (5), 696-704 (2013).
- [22] J. Lellep, E. Puman, Recent Researches in Mechanics: 2nd International Conference on Theoretical and Applied Mechanics, Corfu, Greece, 2011. Edited by N. Mastorakis et al. WSEAS, 223–228.
- [23] J. Lellep, E. Puman, L. Roots, E. Tungal, *WSEAS Transactions on Mathematics*, **9** (2), 130–139 (2010).

Publication IV

Majak, J.; Anton, J.; Õunapuu, E.; Auriemma, F.; Pohlak, M.; Eerme, M.; Klauson, A. (2019). Experimental Evaluation and Numerical Modelling Residual Stresses in Glass Panel. MATEC Web Conferences; 253.

Experimental Evaluation and Numerical Modelling Residual Stresses in Glass Panel

Jüri Majak^{1,a}, Johan Anton^{3,4}, Erko Õunapuu¹, Fabio Auriemma¹, Meelis Pohlak¹, Martin Eerme¹ and Aleksander Klauson²

¹Department of Mechanical and Industrial Engineering, Tallinn University of Technology, 19086, Tallinn, Estonia

²Department of Civil Engineering and Architecture, Tallinn University of Technology, 19086, Tallinn, Estonia

³Department of Cybernetics, Tallinn University of Technology, 19086, Tallinn, Estonia

⁴GlasStress Ltd, 12618, Tallinn, Estonia

Abstract. During last decade increased usage of laminated composite glass structures, also annealed and tempered glass can be observed in civil engineering, automobile and space structures, solar panels, etc. Latter trend is caused by high strength properties of laminated glass, also sound and vibration attenuation capabilities. However, heat treatment of glass causes residual stresses, which are not often covered in structural analysis. Current study is focused on experimental evaluation and numerical modelling of residual stresses in glass panels.

1 Introduction

The non-destructive testing methods are preferred as resource saving and sustainable. The PVB interlayers have key role in aging of LGCP laminates and need special attention since in a number of application long term exploitation of LGCP panels has been foreseen (solar panels, windows). The elastic material properties of the PVB interlayer determined experimentally are used as simulation input parameters in order to predict vibration attenuation capability at concurrent frequency excitation and displacement.

The main advantage of the laminated glass composite panel, over float glass is its high strength properties, especially fact that it does not break into small pieces even in the case of impact loading cases [1]. The residual stresses arise in glass during cooling down from the crystallization temperature. The residual stresses are caused by the thermal expansion and the elastic mismatch between the crystalline and glassy phases [2,3]. The strengthening effect is achieved with accurate cooling the glass after heat treatment. The fast cooling causes outer layers of the glass to compress and close micro cracks in the surface of the glass. The heat treated glass is used in applications with safety glass requirements [4]. The heat treated glass, especially laminated glass composite panels (LGCP) are used in structures where glass is the main load bearing element. The LGCP consists of glass layers and at least one flexible interlayer. The interlayer provides higher post failure safety of LGCP due to ability to hold broken-off pieces of glass together [5]. Multifunctional LGCP with improved strength and acoustic performance can be obtained by using novel acoustic interlayers covering strengthening and

^a Corresponding author : juri.majak@taltech.ee

sound attenuation properties simultaneously. Development of new sound absorptive element for wide class of structures and applications is emerging research area [6-9].

In the current study an attempt is made to combine the know-how and capabilities of the private company GlasStress Ltd in area of experimental study of residual stresses in glass structures [10-12] and optimization workgroup of TTU (Tallinn University of Technology) in area of structural analysis and design optimization [13-17].

2 Experimental study

The experimental study performed cover evaluation of residual stresses in glass, also measuring the properties of the constituents of glass laminate composite panel for use in further numerical analysis.

2.1 Residual stresses in glass

2.1.1 Measuring residual stresses

Measuring residual stresses has been conducted in private company GlasStress Ltd according to proposed design of experiment. The SCALP-05 and scattered light method were used to determine through-the-thickness stress distribution of annealed and heat treated sodalime glass panels. Three repeatable measurements were done in directions of the long and short sides of the panel at 10 different locations panel. The residual stresses were measured on both sides up to middle surface of the glass panel. The tin side of the glass was detected by employing Tin Side Detector UV1301. The samples tested were 500x200 mm with thicknesses: 4mm, 8 mm and 4+4 mm laminated glass with 0,38 mm PVB interlayer. Through-the-thickness distribution of the stress component σ_1 is given in Figure 1.

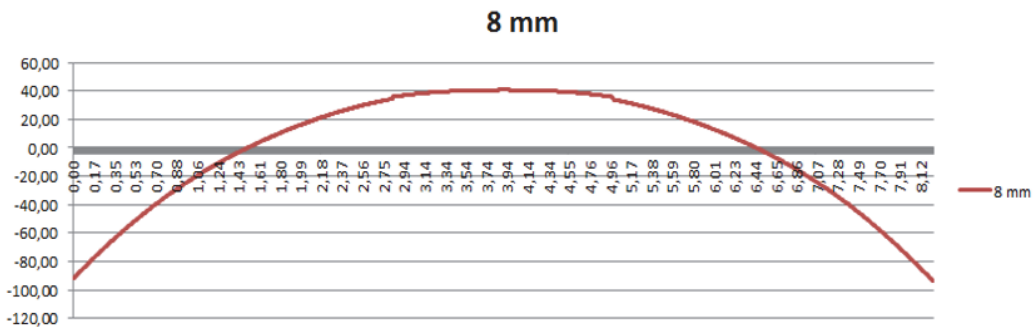


Figure 1. Normal stress component σ_1 - through-thickness distribution

Similarly, symmetric through-the-thickness distribution of the normal stress component σ_2 has been observed. The experimental data obtained, provide valuable information on behaviour of residual stresses in glass panel. However, these data are not enough for numerical modelling of residual stresses in glass panel due to presence of normal stress components only. Solution of the latter problem is discussed in the following section.

2.1.2 Determining shear stresses in laminated glass

In order to evaluate the shear stresses σ_{12} in glass panel the procedure based on measurement of normal stresses in different rotation angles and application of the plane stress tensor rotation formulas is introduced. The procedure is given as follows:

- The initial coordinate system was specified by long and short sides of the glass specimen;
- The stress components $\sigma_1^{\text{exp}_0}$ and $\sigma_2^{\text{exp}_0}$ were measured in coordinate system rotated 0° ;

- The stress components $\sigma_1^{\text{exp}_\theta}$ and $\sigma_2^{\text{exp}_\theta}$ were measured in coordinate system rotated θ° ;
- Based on values of the stress components $\sigma_1^{\text{exp}_0}$ and $\sigma_2^{\text{exp}_0}$ the theoretical expected values of the stress components in coordinate system rotated θ° were computed by employing stress tensor rotation formulas as

$$\sigma_1^{\text{theoret}_\theta} = \sigma_1^{\text{exp}_0} \cos^2(\theta) + \sigma_2^{\text{exp}_0} \sin^2(\theta) + 2\sigma_{12}^0 \sin(\theta) \cos(\theta), \quad (1)$$

$$\sigma_2^{\text{theoret}_\theta} = \sigma_1^{\text{exp}_0} \sin^2(\theta) + \sigma_2^{\text{exp}_0} \cos^2(\theta) - 2\sigma_{12}^0 \sin(\theta) \cos(\theta), \quad (2)$$

- Note that the formulas (1)-(2) are not directly applicable, since the value of the shear stress σ_{12}^0 is unknown. For this reason the shear stress σ_{12}^0 was considered as design variable and the differences between experimentally measured normal stresses $\sigma_1^{\text{exp}_\theta}$, $\sigma_2^{\text{exp}_\theta}$ and theoretically computed normal stresses $\sigma_1^{\text{theoret}_\theta}$, $\sigma_2^{\text{theoret}_\theta}$ were subjected to minimization

$$f = (\sigma_1^{\text{theoret}_\theta} - \sigma_1^{\text{exp}_\theta})^2 + (\sigma_2^{\text{theoret}_\theta} - \sigma_2^{\text{exp}_\theta})^2 \rightarrow \min. \quad (3)$$

- Applying the necessary optimality conditions for posed optimization problem $\frac{\partial f}{\partial \sigma_{12}^0} = 0$, the value of the shear stress σ_{12}^0 in initial coordinate system was determined as

$$\sigma_{12}^0 = \frac{(\sin^2(\theta) - \cos^2(\theta))(\sigma_1^{\text{exp}_0} - \sigma_2^{\text{exp}_0}) + (\sigma_1^{\text{exp}_\theta} - \sigma_2^{\text{exp}_\theta})}{4 \sin(\theta) \cos(\theta)}. \quad (4)$$

Note, that the proposed approach is based on measuring residual stresses in two different angles of the coordinate system and is just one possibility for estimating the value of the shear stress σ_{12}^0 . Obviously, the result depends on selection the value of the rotation angle θ . The theoretical approach introduced can be simply extended for a number of rotations of the stress tensor by angles θ_1 to θ_n . However, in latter case the cost needed to pay for higher accuracy is higher number of experiments (the normal stresses should be measured for each value of θ_i).

2.1.3 Error estimate

Having the measured values of the normal stresses $\sigma_1^{\text{exp}_0}$, $\sigma_2^{\text{exp}_0}$ in initial coordinate system and corresponding estimate on shear stress σ_{12}^0 one can apply the stress tensor rotation formulas (1)-(2) for computing the theoretical values of normal stresses $\sigma_1^{\text{theoret}_\theta}$ and $\sigma_2^{\text{theoret}_\theta}$ in new, rotated coordinate system. The errors e_1 and e_2 of the measured normal stresses σ_1 and σ_2 can be estimated as

$$e_1 = \sigma_1^{\text{exp}_\theta} - \sigma_1^{\text{theoret}_\theta}, \quad (5)$$

$$e_2 = \sigma_2^{\text{exp}_\theta} - \sigma_2^{\text{theoret}_\theta}. \quad (6)$$

It should be noted that e_1 and e_2 are caused by measuring errors in both coordinate systems (initial and rotated by angle θ). Based on formulas (5)-(6) the error of residual stresses near outer surface (biggest values of stresses) are estimated $\sim 1\text{MPa}$ (near 1%).

2.2 Properties of glass layer – non-destructive testing

In order to perform numerical analysis of glass panel the mechanical properties of the panel should be determined. However, performing traditional mechanical tests with glass specimen is rather complicated, especially tension tests, etc. Furthermore, as mentioned above the non-destructive testing should be preferred. The non-destructive mechanical testing procedure for glass panel was introduced by authors in [18]. The time of flight of the individual pulses has been measured in order to determine sound speeds of P-wave and shear wave. The setup of the test is shown in Figure 2.

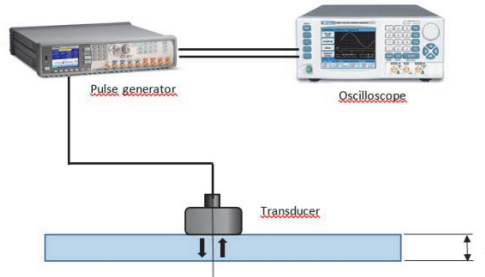


Figure 2. Set up for measuring P-wave and shear wave speeds

The Young modulus and Poisson ratio of the glass can be evaluated as

$$E = \frac{G(3M - 4G)}{M - G}, \quad (7)$$

$$\nu = \frac{M - 2G}{2M - 2G}, \quad (8)$$

where

$$M = c_p^2 \rho, \quad G = c_s^2 \rho, \quad (9)$$

c_p and c_s stand for the wave speeds and ρ is a material density. The wave speeds measured as well as the material properties computed are presented in table 1.

Table 1. Material properties of the glass layer.

	ρ (kg/m ³)	c_p (m/s)	c_s (m/s)	E (GPa)	ν
Float glass	2486	5914	3506	75.11	0.23
Tempered glass	2486	5852	3433	72.53	0.24

The mechanical properties of the PVB interlayer are determined from traditional tensile tests. Due to small thickness and viscoelastic material properties of PVB interlayer the above proposed non-destructive testing is complicated.

3 Numerical modelling

The experimental data acquired by employing procedures introduced in sections 2.1 and 2.2 can be utilized as input data for finite element method (FEM) analysis model. The FE analysis was performed using ANSYS v14.

3.1 FEM model and its validation tests

Modal analysis of glass panels without supports and pre-stress was selected for FE model development and validation. FEA model consists of 50 000 8-noded hexahedral 3D solid elements (8 layers of elements through the thickness of the glass sheet). The FEA and experimental modal analysis has been applied to a glass panel with dimensions 500mm × 200mm × 8mm. The samples are held by a suspension system, constituted by soft elastic bands. These bands are designed to guarantee that the highest rigid mode frequency is less than 10 – 15% of the first resonance frequency of the suspended structure. This circumstance allows considering the systems as in free-free conditions. The classical roving hammer impact test has been used to measure the frequency response functions and to implement the peak-picking method. Preliminarily, a set of points are defined on a wire-frame created on the structure and an accelerometer is fixed on one of these points. The method consists of

measuring the frequency response functions between the response measured by the accelerometer and the forced excitation provided by the hammer when the wire-frame points are sequentially hit. In the present investigation, the samples have been schematized with a wire-frame consisting of 12 points displaced in adjacent rectangular patterns. An impulsive excitation has been provided, along the direction perpendicular to the plane of the structure, by means of a hammer AP Tech™ AU01 provided with force transducer. The vibration response has been measured, along the same direction, by means of an ICP (Integrated Circuit Piezoelectric) mono-axial accelerometer PCB™ TM 353B33. The signal acquisition has been performed by a dynamic signal analyser (National Instruments™ NIcDAQ 9174 and NI 9234), controlled by PC based virtual instrument (LabVIEW™). Random errors have been reduced by averaging out three subsequent measurements taken for each point. The frequency response functions have been estimated as $H = S_{XY} / S_{XX}$, i.e. as the ratio of the cross-spectrum of excitation and response signals over the auto-spectrum of the excitation signal (Figure 3).

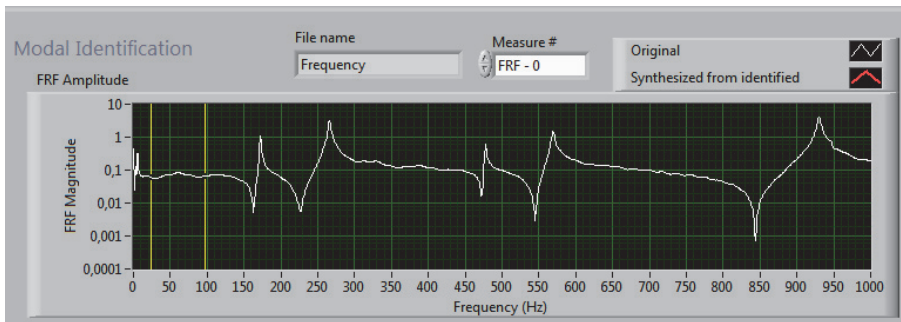


Figure 3. FRF Magnitude vs frequency.

The values of the coherence function related to the impact tests, are above 98%, indicating low levels of uncorrelated noise in the measured frequency response data. In Table 2 the values of the natural frequencies obtained from FEM analysis and experimental tests are presented.

Table 2. Frequency values. FEM vs experimental.

Mode	Frequency, Hz FEM model	Frequency, Hz Experimental
1	172	172
2	267	266
3	477	477
4	571	569
5	930	930

One can be observed from Table 2 that the results obtained from experimental study and FEM analysis are in good agreement.

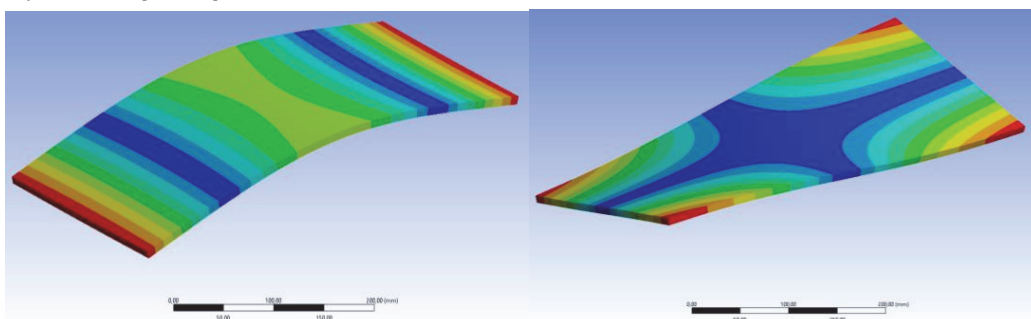


Figure 4. Fundamental frequency and second harmonic.

The fundamental frequency and second harmonic are depicted in Figure 4.

3.2 Modelling residual stresses in glass

Glass panel with size 200x500x8 mm and material properties described above was considered. In order to apply pre-stress one side of panel was fixed (short side is fixed) i.e. console. The values of the stress tensor obtained from experimental study (normal stresses σ_1 and σ_2) and from procedure proposed in section 2.1.2 (shear stress σ_{12}) are mapped into FEA model by ANSYS throughout the thickness in 57834 points (Figure 5).

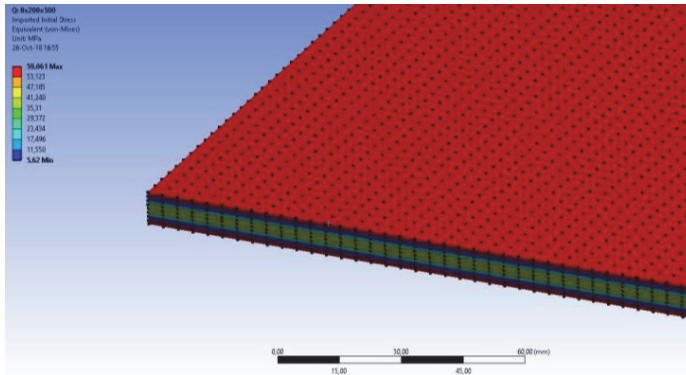


Figure 5. Mapped stresses.

The results of modal analysis are given in Table 3.

Table 3. Frequency values, with and without pre-stress

Mode	Frequency, Hz without pre-stress	Frequency, Hz with pre-stress
1	27	28
2	145	150
3	171	174
4	461	476
5	480	489

It can be observed from Table 3 that in the case of considered boundary conditions (console type, short side fixed) the influence of residual stresses on frequency values is remarkable. Application of residual stresses increase the values of the frequencies. The modes corresponding to first two frequencies are depicted in Figure 6.

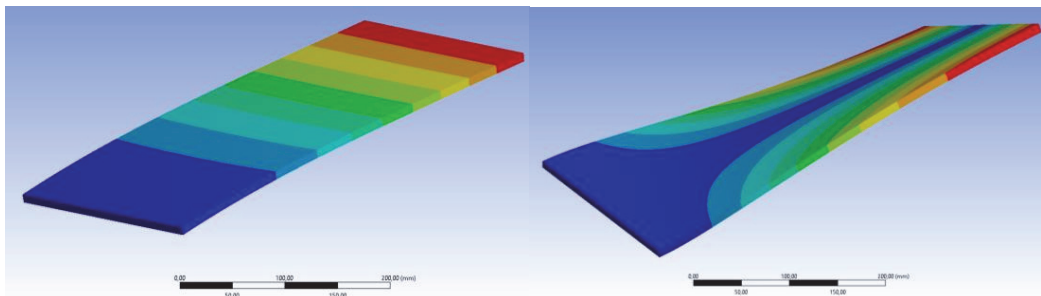


Figure 6. Fundamental frequency and second harmonic for pre-stressed panel.

Figure 6 is obtained by applying console type boundary conditions where short side of the panel is fixed.

4 Conclusions

An approach for structural analysis the glass panels, incorporating residual stresses, has been proposed. The normal residual stresses were determined experimentally in private company GlasStress Ltd. The procedure for determining shear stress component of residual stress tensor has been developed. The algorithm for estimating error of the measured residual stresses has been introduced. The finite element model incorporating residual stresses has been developed. The remarkable influence of the residual stresses on values of the natural frequencies has been observed. An approach proposed for structural analysis can be applied for wide class of glass structures. Future study planned cover design optimization of laminated glass composite panel [19-23].

Acknowledgments

The authors acknowledge Innovative Manufacturing Engineering Systems Competence Centre IMECC (co-financed by the project EU48685); the Estonian Centre of Excellence in Zero Energy and Resource Efficient Smart Buildings and Districts, ZEBE, TK146 funded by the European Regional Development Fund (grant 2014-2020.4.01.15-0016); Estonian Research Council grant PUT1300.

References

1. M. Haldimann, A. Luible A and M. Overend, Structural Engineering Documents, 10. IABSE, Zürich (2008).
2. M. Kotoul, J. Pokluda, P. Sandera, I. Dlouh?, Z. Chlup, A.R. Boccaccini, Acta Mater., **56**, 2908-2918 (2008).
3. F.C. Serbena, E.D. Zanotto, Journal of Non-Crystalline Solids, **358**, 6-7, 975-984 (2012).
4. M. Fröling, *Strength Design Methods for Glass Structures*, Doctoral Thesis (2013).
5. X. Zhang H. Hao, Construction and Building Materials, **93**, 404-415 (2015).
6. F. Auriemma, H. Rammal, J. Lavrentiev, SAE Int. J. of Materials and Manufacturing, **1**,1, 600-611 (2014).
7. F. Auriemma, Applied Acoustics, **122**, 128-137 (2017).
8. F. Auriemma, Acoustics Australia, **45**, 2, 411-419 (2017).
9. F. Auriemma, Proc. of Meetings on Acoustics Meeting of Acoust. Society of America, **30**, 1 (2017).
10. S. Hödemann, A. Valdmann, J. Anton, T. Murata, J. of Materials Sci., **51**,12 (2016).
11. H. Aben, J. Anton, M. Õis, K. Viswanathan, C. Chandrasekar, M. M. Chaudhri, App. Physics Letters, **109**, 231903 (2016).
12. H. Aben, D. Lochegnies, Y. Chen, J. Anton, M. Paemurru, M. Õis, Experim. Mech., **55**, 2, 483-486 (2015).
13. J. Lellep, J. Majak, Struct. Optimization, **14**, 116-120 (1997).
14. J. Lellep, J. Majak, Mech. of Composite Materials, **36**, 4, 261-266 (2000).
15. A. Aruniit, J. Kers, J. Majak, A. Krumme, K. Tall, Proc. of Estonian Acad. of Sci., **61**, 3, 160-165 (2012).
16. A. Aruniit, J. Kers, D. Goljandin, M. Saarna, K. Tall, J. Majak, H. Herranen, Materials Science (Medžiagotyra), **17**, 3, 276-281 (2011).
17. J.Majak, S.Hannus, Mech. of Composite Materials, **39**, 6, 509-520 (2003).
18. K.Väer, J. Anton, A. Klauson, M. Eerme, E. Õunapuu, P. Tšukrejev, Journal of Achievements in Materials and Manufacturing Engineering, **81**,1, 11-17 (2017).
19. J. Šlisseris, K. Rocens, World Acad. of Sci., Eng. and Tech., **76**, 317-323 (2011).
20. J. Šlisseris, K. Rocens, J. of Civil Eng. and Management, **19** (5), 696-704 (2013).
21. W.H.Zhang, M. Domaszewski, D. Bassir, Structural Optimization, **17**, 2, 219-225 (1999).
22. S. Guessasma, D. Bassir, L. Hedjazi, Materials and Design, **65**, 1053-1063 (2015).
23. J.Zhu, W. Zhang, L. Xia, Q. Zhang, D. Bassir, Journal of Intelligent and Robotic Systems: Theory and Applications. **67**, 3-4, 185-199 (2012).

Curriculum vitae

Personal data

Name: Erko Õunapuu
Date of birth: 29.04.1988
Place of birth: Põltsamaa
Citizenship: Estonian

Contact data

E-mail: erkoounapuu1@gmail.com

Education

2013–2019 Tallinn University of Technology – PhD
2011–2013 Tallinn University of Technology – MSc
2007–2011 Tallinn University of Technology – BSc
2004–2007 Põltsamaa Ühisgümnaasium – High school

Language competence

Estonian Native speaker
English Very good
German Good
Russian Basic

Professional employment

2012–2019 R-FIX OÜ – Development Engineer

Elulookirjeldus

Isikuandmed

Nimi: Erko Õunapuu
Sünniaeg: 29.04.1988
Sünnikoht: Põltsamaa
Kodakondsus: Eesti

Kontaktandmed

E-post: erkoounapuu1@gmail.com

Hariduskäik

2013–2019 Tallinna Tehnikaülikool – PhD
2011–2013 Tallinna Tehnikaülikool – MSc
2007–2011 Tallinna Tehnikaülikool – BSc
2004–2007 Põltsamaa Ühisgümnaasium – Keskharidus

Keelteoskus

Eesti keel Emakeel
Inglise keel Väga hea
Saksa keel Hea
Vene keel Algtase

Teenistuskäik

2012–2019 R-FIX OÜ - Arendusinsener

